Feng *et al. Alzheimer's Research & Therapy* (2025) 17:102
https://doi.org/10.1186/s13195-025-01743-5

Alzheimer's Research & Therapy

RESEARCH Open Access

Linking oxysterols and different stages of mild cognitive impairment: insights from gut metabolites and N6-methyladenosine

Wenjing Feng[1], Mengwei Ju[1], Tao Wang[1], Shanshan Cui[1], Kexin Yang[1], Zhiting Guo[1], Miao Liu[1], Jiaxuan Tao[1], Huiyan Yu[1] and Rong Xiao[1*]

Abstract

Background Oxysterols, gut metabolites, and N6-methyladenosine (m6A) are extensively implicated in the pathogenesis of cognitive dysfunction, while their alterations in different stages of mild cognitive impairment (MCI) have not been elucidated. Therefore, this study was conducted to explore the associations of oxysterols, gut metabolites, and m6A methylation profiles in early MCI (EMCI) and late MCI (LMCI) individuals.

Methods Liquid chromatography-mass spectrometry, untargeted metabolomic analysis, and m6A mRNA Epitranscriptomic Microarray were used to detect the characteristics of serum oxysterols ($n=35$/group), fecal gut metabolites ($n=30$/group), and m6A in whole blood ($n=4$/group) respectively. The concentration of serum β-amyloid (Aβ) was detected with ELISA ($n=25$/group). The gene expression of amyloid precursor protein (APP) and its key enzyme β-secretase (BACE1) in whole blood were measured by quantitative real-time PCR ($n=25$/group).

Results EMCIs and LMCIs, especially LMCIs, exhibited poorer performance in almost all global and multidimensional cognitive tests. Serum 27-hydroxycholesterol (27-OHC) and 24S-hydroxycholesterol (24S-OHC) were elevated in EMCI and LMCI groups. Changes in gut metabolites occurred mainly in the EMCI group, in which several gut metabolites, including Procyanidin dimer B7 and Phorbol myristate, were significantly decreased. The m6A methylation landscape of EMCIs and LMCIs obviously differed from Controls. Hypomethylated mRNAs accounted for the majority and were mainly accompanied by downregulated mRNAs, which was consistent with the downregulated expression of the m6A writer methyltransferase-like 4 (METTL4). 27-OHC and 24S-OHC combined with various gut metabolites significantly distinguished between MCI subgroups from healthy controls (EMCI/Control: AUC = 0.877; LMCI/Control: AUC = 0.952). Heatmap revealed the correlation between Phorbol myristate and differentially m6A-methylated mRNAs. Differentially expressed gut metabolites and methylated mRNAs were commonly enriched in 34 KEGG metabolic pathways, including cholesterol metabolism and neurodegenerative disease-related pathways.

Conclusions Our study explored the altered oxysterols, gut metabolites, and m6A methylation and their associations in different stages of MCI. The potential function of aberrant gut metabolites in oxysterols and m6A methylation driving MCI progression warrants further mechanistic investigation.

*Correspondence:
Rong Xiao
xiaor22@ccmu.edu.cn; xrccmu_tg@126.com

Full list of author information is available at the end of the article

Keywords Mild cognitive impairment, Oxysterols, Gut metabolites, N6-methyladenosine, Cognitive assessment

Introduction

Mild cognitive impairment (MCI), as the transitional stage of Alzheimer's disease (AD), is characterized by a complex cognitive syndrome between normal aging and dementia without notable interference with activities of daily life [1]. Based on the degree of cognitive dysfunction, MCI is subcategorized into early MCI (EMCI) and late MCI (LMCI), with the latter characterized by a more severe cognitive decline [2]. Among the various risk factors for MCI, cholesterol homeostasis and its oxidative metabolites, oxysterols, have been widely demonstrated to contribute to the development of cognitive impairment [3]. In particular, 27-hydroxycholesterol (27-OHC), the prominent oxysterol in peripheral circulation, has been demonstrated to remarkably increase in the blood of MCI patients in our previous studies, following higher serum concentrations of amyloid-β (Aβ) [4, 5]. However, the alteration of oxysterols and Aβ in the comparison of EMCI and LMCI deserves to be further explored.

Disordered gut microbiota has been confirmed to be one of the key mechanisms of cognitive dysfunction, and theories related to gut microbiota and metabolites are gradually improved [6]. The specific changes in the gut microbiota profile of MCI subjects have been described comprehensively in our previous study [7]. A wide variety of gut microbiota can produce multitudinous metabolites to exert neuroprotective or neurodamaging functions, such as bile acids, short-chain fatty acids (SCFAs), amino acids, and so on [8]. A large number of gut metabolites have been screened by metabolomics [9]. However, what are the characteristics of gut metabolite profiles in individuals with different cognitive levels? In our published research, disturbed gut metabolites were detected in mice with impaired learning and memory induced by 27-OHC [10]. However, whether there is an association between gut metabolites and oxysterols in the progression of MCI has not been well elucidated, which is another question to be explored in this study.

N6-methyladenosine (m6A), the most usual and abundant eukaryotic methylation in RNA, contributes to RNA splicing and degradation, translation, and nuclear export [11]. The dynamic modification of m6A is regulated by writer (methyltransferases), eraser (demethylases), and reader (methylation-binding proteins) [12]. Among them, methyltransferase-like 4 (METTL4), one of the methyltransferases, has been proven to be decreased in the brain of 27-OHC-treated mice, followed by memory decline [13]. The specific changes of m6A methylation in AD have gradually attracted attention [14–16]. Besides, some gut metabolites, such as bile acids, have been discovered to regulate the landscape of host m6A epitranscriptome directly through their metabolism pathway [17]. Another gut metabolite, butyrate, was also found to alter the expression of m6A methylated mRNA, which has proven the tight connection between gut metabolites and m6A methylation [18]. In fact, the specific alteration of m6A methylation in EMCI and LMCI subjects and its association with gut metabolites remain unclear.

This case-control study was conducted to explore the alteration in oxysterols with the risk of EMCI and LMCI, to confirm the metabolic spectrum of gut metabolites and transcriptome-wide profile of m6A that specifically are altered in individuals with different cognitive levels, and to excavate the potential correlation of oxysterols, gut metabolites, and m6A methylation in the progression of different stages of MCI. Our study aims to provide new supporting evidence for early detection and intervention of microbial and epigenetic regulators in the development of cognitive impairment.

Methods

Study population

The study subjects were recruited from a prospective, multicenter cohort consisting of community-dwelling volunteers aged 50 ~ 75 years in Shanxi Province, China. Based on the detailed inclusion and exclusion criteria described earlier [7], 367 Controls, 312 EMCI participants, and 244 LMCI participants were included. Face-to-face interviews were conducted to collect demographic data, lifestyle information, and chronic medical history, as well as the outcomes of tests measuring global and multidimensional cognitive function. Fasting peripheral blood was drawn. From this, one tube was centrifuged after coagulation to collect serum, followed by subpackaging and storage at -80 °C. The remaining 2 mL of fresh whole blood (EDTA- anticoagulated) was immediately mixed with three volumes of RNA LOCK reagent (TIANGEN, DP440) to protect RNA. The mixed system was lysed for 2 h at room temperature before being stored at -80℃, and RNA was extracted within 6 months to carry out m6A detection and quantitative real-time PCR (RT-qPCR). On the same day, fresh fecal samples were collected immediately and stored at -80℃ until detected. The experiment was approved by the Ethics Committee of Capital Medical University (Z2023SY024) in accordance with the Declaration of Helsinki, with signed informed consent from all individuals before each examination.

Cognitive assessment

Both global and multidimensional cognitive functions were measured. The former was evaluated by standard

cognitive tests, including the Mini-Mental State Examination (MMSE) and Montreal Cognitive Assessment (MoCA). As for multidimensional cognitive function, simply put, the Auditory Verbal Learning Test (AVLT), which consisted of immediate recall (AVLT-IR), short recall (AVLT-SR), and long recall (AVLT-LR) was carried out to assess verbal memory function [19]. The processing speed was evaluated through the symbol digit modalities test (SDMT) [20], while executive function and attention were measured by the logical memory test (LMT) [19]. Besides, digit span forwards (DSF) and digit span backwards (DSB) were used to estimate working memory [19]. Trail making test-A (TMT-A) and B (TMT-B) evaluated visual-spatial attention and divided attention, respectively [21]. The Stroop color-word tests (SCWT), including reaction interference effects (SCWT-RIE) and time interference effects (SCWT-TIE) were conducted to assess cognitive flexibility [22].

Diagnosis of EMCI and LMCI

First, subjects underwent MoCA and MMSE tests. The full scores for both MoCA and MMSE were 30 points. The MoCA screening threshold score was ≤14 points for illiteracy, ≤ 19 points for 1–6 years of education, and ≤24 points for 7 years of education and above [7]. Individuals initially identified as suspected MCI were further confirmed by neurologists. MCI individuals who scored ≥24 points on the MMSE were further divided into EMCI and LMCI depending on Wechsler Memory Scale-recall (WMS-R) test, which was the recall of LMT after an interval of 10 min. Specifically, the EMCI criteria were 3–6 points for 0–7 years of education, 5–9 points for 8–15 years, and 9–11 points for 16 years or more. For LMCI subjects, the score was ≤2 for those with 0–7 years of education, ≤ 4 for those with 8–15 years of education, and ≤8 for those with 16 years or more of education [23].

Lipids and oxysterols detection

Serum lipids, including total cholesterol (TC), triglyceride (TG), high-density lipoprotein cholesterol (HDL-C), and low-density lipoprotein cholesterol (LDL-C) were measured by an automatic biochemistry analyzer (Roche Hitachi 8000 C). Liquid chromatography-mass spectrometry (LC-MS) was utilized to detect the serum concentration of oxysterols according to the published protocols [24].

Gut metabolites identification

Untargeted LC-MS metabolomic analysis was performed to characterize different metabolites and the related biochemical pathways among groups ($n = 30$ per group, the statistics of the characteristics were shown in TableS1-S3). In brief, The metabolites from fecal samples were extracted from a methanol aqueous solution (methanol: water = 4:1, v: v) containing 0.02 mg/mL internal standard (L-2-chlorophenylalanine). The sample was separated using an HSS T3 column (100 mm× 2.1 mm i.d., 1.8 μm) and then detected by mass spectrometry. The original data of LC-MS were imported into the metabonomics processing software Progenesis QI (Waters Corporation, Milford, USA) for filtering and identification, resulting in the creation of a data matrix. Finally, data were uploaded to the Majorbio cloud platform (https://cloud.majorbio.com) for analysis. Differential metabolites were identified when they met the conditions of Variable Importance in Projection (VIP) > 1, $P < 0.05$ (adjusted via Scheffé test) based on the VIP obtained by the orthogonal least partial squares discriminant analysis (OPLS-DA) model and the *P*-value generated by Student's t-test in pairwise comparison. Furthermore, different metabolites were mapped into their biochemical pathways through metabolic enrichment and pathway analysis based on the KEGG database.

m6A methylation detection

m6A modification was detected through m6A mRNA Epitranscriptomic Microarray by Aksomics Inc., (Shanghai, China) ($n = 4$/group, the statistics of the characteristics were shown in Table S4-S6). Briefly, the total RNAs of samples were immunoprecipitated with anti-m6A antibody, in which the modified RNAs were eluted as the "IP", while unmodified RNAs were recovered from the supernatant as "Sup". The "IP" and "Sup" RNAs were labeled with Cy5 and Cy3 respectively as cRNAs in separate reactions using Arraystar RNA Labeling Protocol. The cRNAs were combined and hybridized onto Arraystar Human mRNA Epitranscriptomic Microarray (8 × 60 K, Arraystar). After washing the slides, the arrays were scanned in two-color channels by an Agilent Scanner G2505C.

Agilent Feature Extraction software (version 11.0.1.1) was used to analyze the obtained array images. Raw intensities of IP and Sup were normalized with an average of log2-scaled Spike-in RNA intensities. After Spike-in normalization, the probe signals having Present (P) or Marginal (M) QC flags in at least 4 out of 24 samples were retained for further "m6A quantity" analyses, which was calculated for the m6A modification amount based on the IP normalized intensities. Differentially m6A-modified RNAs between two comparison groups were identified by filtering with the fold change and statistical significance (*P*-value, adjusted by FDR) thresholds. Hierarchical Clustering was performed to show the distinguishable m6A-modification pattern among samples.

The gene expression of m6A and Aβ related enzymes

The serum expression levels of m6A-modifying enzyme and cognitive biomarkers were detected by RT-qPCR. The specific primers used in this study are presented in

Table 1 Primers used in this study for RT-qPCR

Primer	Forward sequence (5′-3′)	Reverse sequence (5′-3′)
m6A modifying enzymes		
METTL3	CTATCTCCTGGCACTCGCAAGA	GCTTGAACCGTGCAACCACATC
METTL4	AGTGCCGACAGCATTGGTG	GGAGCAGAGGTATCATAGGAAGC
FTO	TTGGACGGTACAGATATGGAACATTTT	TCTTTTAGTTTCTTTGCCTTTGGGGAT
ALKBH5	CCAGCTATGCTTCAGATCGCCT	GGTTCTCTTCCTTGTCCATCTCC
Cognitive biomarkers		
APP	ATGCTGCCCGGTTTGGCA	CTAGTTCTGCATCTGCTCAAAGAACTTG
BACE1	TACCAACCAGTCCTTCCGC	CTCCCATAACAGTGCCCGT
β-actin	AAGTGTGACGTTGACATCCG	GATCCACATCTGCTGGAAGG

Abbreviations: METTL3, methyltransferase-like 3; METTL4, methyltransferase-like 4; FTO, fat mass and obesity-associated; ALKBH5, AlkB homolog 5; APP, amyloid precursor protein; BACE1, β-secretase

Table 2 Demographic data of control, EMCI, and LMCI subjects

Variables	Control	EMCI	LMCI	*P*	Adjusted *P* value for pairwise comparisons
Male, n (%)	153 (41.7)	132 (42.3)	101 (41.4)	0.051[2]	
Age, y	65 ± 8	65 ± 8	65 ± 7	0.153[1]	
Education year, y	12 ± 3	9 ± 3	9 ± 3	**0.006**[1]	LMCI < Control *P* = 0.005
Smoker, n (%)	84 (22.9)	87 (27.9)	63 (25.8)	0.323[2]	
Drinker, n (%)	88 (24.0)	69 (22.1)	54 (22.1)	0.806[2]	
Hypertension, n (%)	131 (35.7)	126 (40.4)	102 (41.8)	0.254[2]	
Diabetes, n (%)	66 (18.0)	76 (24.4)	42 (17.2)	0.054[2]	
Hyperlipemia, n (%)	113 (30.8)	103 (33.0)	90 (36.9)	0.292[2]	
CHD, n (%)	35 (9.5)	43 (13.8)	36 (14.8)	0.101[2]	

[1] *P* value for Kruskal-Wallis rank sum test for continuous variables with skewed distribution, which were presented as medians ± interquartile range. Adjusted *P* value by Bonferroni correction

[2] *P* value for Chi-square tests for categorical variables, which were presented as n (%)

Abbreviations: EMCI, early mild cognitive impairment; LMCI, late mild cognitive impairment; CHD, coronary heart disease

Table 1. Total RNA was extracted using RNAprep pure high-efficiency total RNA extraction kit (TIANGEN, DP443) in strict accordance with the manufacturer's procedures. RT-qPCR experiments were performed using the KAPA SYBR® PCR kit (Kapa Biosystems, Woburn, MA, USA). A minimum of three experiments were performed for each sample.

The concentrations of serum Aβ and oxidized lipoproteins

The concentrations of Aβ (Elabscience, E-EL-H0543), oxidized LDL (ox-LDL) (Elabscience, E-EL-H6021), and oxidized HDL (ox-HDL) (JINGMEI, JM-7052H1) in serum were quantified by ELISA Kit based on the manufacturer's instructions.

Statistical analysis

All data were analyzed by R4.3.3, IBM SPSS 23.0, OriginPro 2024, and GraphPad Prism 9 software. Demographic and biochemical measures were expressed as means ± standard deviations or medians ± interquartile ranges, depending on the type of data distribution. Differences between groups were compared using one-way ANOVA, Kruskal-Wallis rank sum test, or chi-square test. Logistic regression analysis and receiver operating characteristic (ROC) curve were used to distinguish different stages of MCI by oxysterols and gut metabolites. Differentially methylated mRNAs among the groups were chosen to further screen the altered methylated transcripts based on the value of fold change (FC), in which the top 5 mRNAs with the largest absolute values of $\log_{10}$ (FC) were selected for subsequent analysis. Spearman correlation analysis was conducted to evaluate the correlation between gut metabolites and differentially methylated mRNAs. $P < 0.05$ was considered to indicate statistical significance.

Results

Study population characteristics

Demographic characteristics are presented in Table 2. A significant difference was observed in education years. It was found that individuals in the LMCI group had fewer years of education than the Control group ($P = 0.005$), suggesting the remarkable effect of educational qualifications on cognition. No difference was found in the factors of gender, age, smoker or drinker, as well as the history of chronic diseases such as hypertension, diabetes, hyperlipemia, or coronary heart disease (CHD).

Cognitive functions tests and indicators in EMCI and LMCI participants

As shown in Table 3, all cognitive tests in the global and multidimensional domains exhibited significant variations. Specifically, lower scores on MMSE and DSB tests, along with higher scores on SCWT-TIE and SCWT-RIE tests were found in EMCIs and LMCIs compared with the Control group ($P < 0.001$). In addition, the scores for MoCA, WMS-R, AVLT-IR, AVLT-SR, AVLT-LR, SDMT, LMT, and DSF decreased remarkably in order from the Control, EMCI to LMCI groups. Similarly, the duration of TMT-A and TMT-B tests increased from the Control group, EMCI group to the LMCI group ($P < 0.001$). All the test results indicated that, although EMCI and LMCI were only defined by MoCA and WMS-R tests, both EMCI and LMCI subjects exhibited varying degrees of multi-domain cognitive impairment, where LMCIs performed worse in most tests.

Besides, Aβ serum concentration, mRNA expression level of amyloid precursor protein (APP), and its rate-limiting enzyme β-secretase (BACE1) were detected. As shown in Fig. 1A-C, the serum level of Aβ in the LMCI group increased in comparison with the Control and EMCI groups ($P = 0.002$), which was consistent with the worse cognitive function results in the LMCI group. The expression of APP, which is the precursor of Aβ, was lower in the EMCI group than in the Control group ($P = 0.007$), but there was an increasing trend in the LMCI group compared with the EMCI group.

Serum lipids and oxysterols level in EMCI and LMCI participants

Serum lipids and oxysterols were detected, as shown in Table 4. Compared with the Control group, the serum TC ($P = 0.043$) and LDL-C ($P = 0.024$) were higher in the EMCI group. In addition, the levels of 27-OHC in the LMCI ($P = 0.006$) groups were increased, and 24S-OHC concentration in the Control group was lower than those in the EMCI ($P = 0.007$) and LMCI ($P = 0.018$) groups. Serum ox-LDL increased in the LMCI group compared

Table 3 Cognitive tests of control, EMCI, and LMCI subjects

	Control	EMCI	LMCI	P^1	Adjusted *P* value for pairwise comparisons
Global cognition					
MMSE	28 ± 2	27 ± 3	26.5 ± 3	**< 0.001**	EMCI < Control, $P < 0.001$ LMCI < Control, $P < 0.001$
MoCA	26 ± 2	22 ± 3	21 ± 3	**< 0.001**	EMCI < Control, $P < 0.001$ LMCI < Control, $P < 0.001$ LMCI < EMCI, $P = 0.008$
Multidimensional function					
AVLT-IR	15 ± 7	13 ± 5	11 ± 5	**< 0.001**	LMCI < EMCI < Control, all $P < 0.001$
AVLT-SR	5 ± 4	4 ± 3	3 ± 2	**< 0.001**	LMCI < EMCI < Control, all $P < 0.001$
AVLT-LR	5 ± 4	3 ± 4	2 ± 3	**< 0.001**	LMCI < EMCI < Control, all $P < 0.001$
SDMT	36 ± 15	31 ± 13	29 ± 11	**< 0.001**	EMCI < Control, $P < 0.001$ LMCI < Control, $P < 0.001$ LMCI < EMCI, $P = 0.015$
LMT	10.5 ± 5.9	8 ± 3	4 ± 3	**< 0.001**	LMCI < EMCI < Control, all $P < 0.001$
WMS-R	9.5 ± 7	7 ± 2.5	2.5 ± 2	**< 0.001**	LMCI < EMCI < Control, all $P < 0.001$
DSF	8 ± 1	7 ± 2	7 ± 2	**< 0.001**	EMCI < Control, $P = 0.001$ LMCI < Control, $P < 0.001$ LMCI < EMCI, $P = 0.004$
DSB	4 ± 1	4 ± 1	4 ± 1	**< 0.001**	EMCI < Control, $P < 0.001$ LMCI < Control, $P < 0.001$
TMT-A	64.7 ± 33.5	71.4 ± 30.1	81.8 ± 39.4	**< 0.001**	Control < EMCI, $P < 0.001$ Control < LMCI, $P < 0.001$ EMCI < LMCI, $P = 0.004$
TMT-B	178.1 ± 98.8	204.2 ± 92.3	236.0 ± 123.5	**< 0.001**	Control < EMCI < LMCI, all $P < 0.001$
SCWT-TIE	32.5 ± 16.5	39.0 ± 22.8	37.1 ± 20.0	**< 0.001**	Control < EMCI, $P < 0.001$ Control < LMCI, $P = 0.001$
SCWT-RIE	1 ± 2	2 ± 4	2 ± 5	**< 0.001**	Control < EMCI, $P < 0.001$ Control < LMCI, $P < 0.001$

[1] *P* value for Kruskal-Wallis rank sum test for continuous variables with skewed distribution, which were presented as medians ± interquartile range. Adjusted *P* value by Bonferroni correction

Abbreviations: EMCI, early mild cognitive impairment; LMCI, late mild cognitive impairment; MMSE, mini-mental state examination; MoCA, Montreal cognitive assessment; WMS-R, Wechsler memory scale-recall; AVLT-IR, auditory verbal learning test-immediate recall; AVLT-SR, auditory verbal learning test -short recall; AVLT-LR, auditory verbal learning test-long recall; SDMT, symbol digit modalities test; LMT, logical memory test; DSF, digit span forwards; DSB, digit span backwards; TMT-A, trail making test-A; TMT-B, trail making test-B; SCWT-TIE, Stroop color-word test-time interfered effects; SCWT-RIE, Stroop color-word test-reaction interfered effects

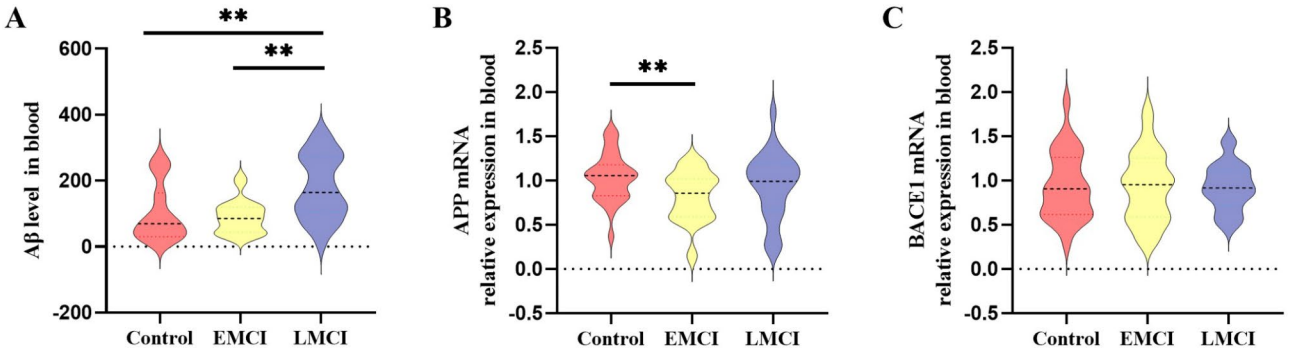

Fig. 1 Cognitive function biomarkers. Aβ (**A**) was analyzed by Kruskal-Wallis rank sum test, while APP (**B**) and BACE1 (**C**) were analyzed by ANOVA test. Abbreviations: EMCI, early mild cognitive impairment; LMCI, late mild cognitive impairment; Aβ, β-amyloid; APP, amyloid precursor protein; BACE1, β-site amyloid cleaving enzyme. *$P < 0.05$, ** $P < 0.01$

Table 4 Serum lipids, lipoproteins, and oxysterols among groups

	Control	EMCI	LMCI	*P*	Adjusted *P* value for pairwise comparisons
TC (mmol/L)	4.60 ± 1.52	4.80 ± 1.50	4.63 ± 1.46	**0.033**[1]	Control < EMCI, $P = 0.043$
TG (mmol/L)	1.42 ± 0.97	1.59 ± 1.01	1.45 ± 0.90	0.184[1]	
HDL-C (mmol/L)	1.22 ± 0.37	1.23 ± 0.44	1.19 ± 0.43	0.315[1]	
LDL-C (mmol/L)	2.48 ± 1.14	2.73 ± 1.10	2.53 ± 1.17	**0.029**[1]	Control < EMCI, $P = 0.024$
ox-LDL (ng/mL)	288.08 ± 183.06	290.83 ± 120.45	305.01 ± 183.96	**0.027**[2]	Control < LMCI, $P = 0.016$ EMCI < LMCI, $P = 0.026$
ox-HDL (ng/mL)	55.27 ± 6.12	59.00 ± 8.61	53.97 ± 18.96	**0.006**[1]	Control < EMCI, $P = 0.009$ LMCI < EMCI, $P = 0.037$
27-OHC (μmol/L)	14.87 ± 4.69	16.21 ± 4.28	17.21 ± 4.14	**0.006**[1]	Control < LMCI, $P = 0.006$
24S-OHC (μmol/L)	23.10 ± 7.41	27.27 ± 8.96	26.19 ± 7.13	**0.004**[1]	Control < EMCI, $P = 0.007$ Control < LMCI, $P = 0.018$
27-CA (μmol/L)	50.40 ± 25.88	41.76 ± 13.49	47.82 ± 19.93	0.345[1]	
7-HOCA (μmol/L)	32.02 ± 27.21	34.30 ± 14.95	35.32 ± 18.60	0.437[1]	

[1] *P* value for Kruskal-Wallis rank sum test for continuous variables with skewed distribution, which were presented as medians ± interquartile range. Adjusted *P* value by Bonferroni correction

[2] *P* value for one way ANOVA test for continuous variables with normal distribution, which were presented as means ± SDs. Adjusted *P* value by LSD correction

Abbreviations: EMCI, early mild cognitive impairment; LMCI, late mild cognitive impairment; TC, total cholesterol; TG, triglyceride; HDL-C, high-density lipoprotein cholesterol; LDL-C, low-density lipoprotein cholesterol; ox-LDL, oxidized low-density lipoprotein; ox-HDL, oxidized high-density lipoprotein; 27-OHC, 27-hydroxycholesterol; 24S-OHC, 24S-hydroxycholesterol; 27-CA, 3β-hydroxy-5-cholestenoic acid; 7-HOCA, 7α-hydroxy-3-oxo-4-cholestenoic acid

with the Control ($P = 0.016$) and EMCI ($P = 0.026$) groups, whereas higher ox-HDL was found in the EMCI group than Control ($P = 0.009$) and LMCI ($P = 0.037$) groups.

Alterations of gut metabolites in EMCI and LMCI participants

To explore the characteristics of gut metabolites in each group, untargeted gut microbiota metabolomics was applied. Firstly, as shown in the Venn diagram (Fig. 2A), 1,128 metabolites were common to the three groups, and 18, 23, and 24 metabolites were specific to the Control, EMCI, and LMCI groups, respectively. Partial Least Squares-Discriminant Analysis (PLS-DA) (Fig. 2B-C) showed the alteration in the gut metabolite profiles in the comparison of Control, EMCI, and LMCI groups. The above results indicated a gut-metabolite shift in different stages of MCI.

To understand the general information of gut metabolites, the metabolites were traced and annotated. Metabolite traceability analysis (Fig. 2D) showed that the amounts of metabolites characterized as host-unique, intestinal-species-unique, as well as shared by host and intestinal species were 28, 30, and 139, respectively. Besides, Kyoto Encyclopedia of Genes and Genomes (KEGG) compound classification identified 74 kinds of metabolites involved in different biological functions, among which 19 kinds of lipids and 10 kinds of steroids were counted, including cholesterol (Fig. 2E). In the results of KEGG pathway, 7 metabolite pathways related to neurodegenerative diseases and 76 metabolite pathways related to lipid metabolism were remarkably enriched (Fig. 2F), implying that the changes of gut metabolites may be potentially related to the abnormality of lipid metabolism and the development of neurodegenerative diseases.

A new set of differential metabolites between groups was used for further analysis. Firstly, it was presented in the volcano plot that there were 70 and 128 differential

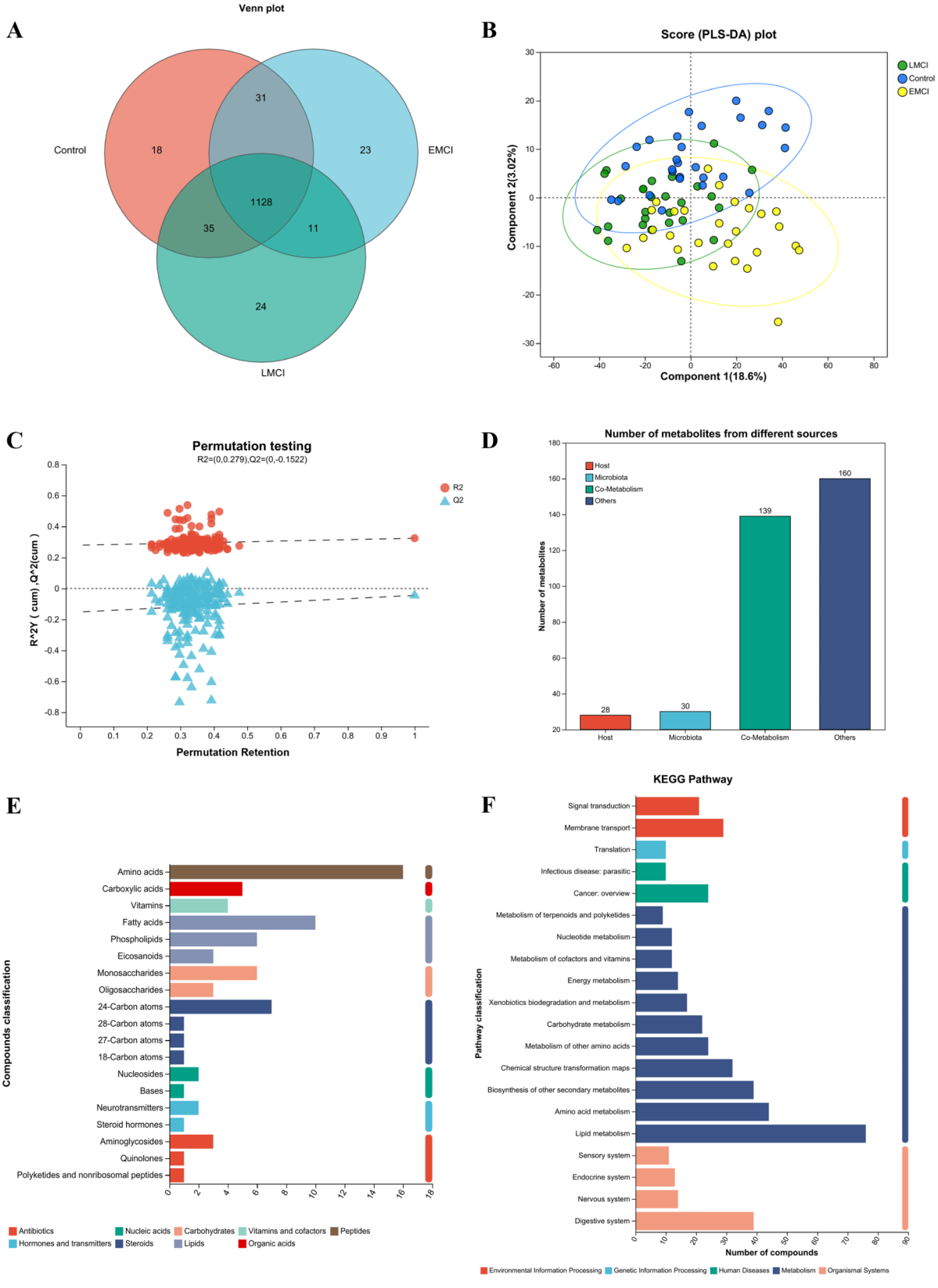

Fig. 2 (See legend on next page.)

(See figure on previous page.)

Fig. 2 Quality analysis and metabolites annotation of metabolomics data in Control, EMCI and LMCI groups. **A**: Venn diagram of the differential metabolites. The overlapping part indicated the same amounts of metabolites among groups. **B**: PLS-DA score plot. The x-axis and y-axis represented the explanatory degree of the first (Component1) and the second (Component2) principal components, respectively. **C**: PLS-DA permutation test was used to verify the fitting effect of the model. The x-axis represented the retention of permutation test, the y-axis represented the values of R2 (red dot) and Q2 (blue triangle) permutation test, and the two dotted lines respectively represented the regression lines of R2 and Q2. **D**: Traceability analysis of metabolites. The x-axis represented the source of metabolites; The y-axis represented the number of metabolites. **E**: KEGG compound classification. The y-axis was KEGG compound classification, and the x-axis was the number of compounds annotated to corresponding types; The color of the bar indicated the primary class of the compound to which they belonged. **F**: KEGG pathway analysis. The y-axis was the secondary classification of KEGG metabolic pathway, and the x-axis was the number of compounds annotated to this pathway

metabolites between the EMCI/Control and LMCI/EMCI groups respectively, while only a few metabolites were altered in the LMCI group compared with the Control group (Fig. 3A-C). In detail, the concentrations of Fasciculic acid B, N2-Fructopyranosylarginine, Thymol-beta-d-glucoside, Thromboxane B2, Phorbol myristate, Procyanidin dimer B7, 2,3-dinor, 6-keto-pgf1alpha, 3-Epipapyriferic acid and Cyclo (Leu-Phe) in EMCI groups were remarkably lower than those in Control and LMCI groups (Fig. 3D). Venn diagram (Fig. 3E) showed that no metabolite was altered together in all three comparisons, but EMCI/Control and LMCI/EMCI had 39 common differential metabolites, suggesting that the metabolite pattern of LMCI was more similar to Control rather than EMCI. VIP scores were used to rank the discriminative contribution of metabolites to each group (Fig. 3F-H). Tumonoic Acid E, Fissinolide, and Pegvaliase were the highest expressed differential metabolites in EMCI/Control, LMCI/Control, and LMCI /EMCI, respectively. In the end, KEGG enrichment analysis showed that neuroactive ligand-receptor interactions were enriched in all comparison groups. In addition, cholesterol metabolism, primary bile acid synthesis, and Huntington's disease were enriched in EMCI/LMCI, while steroid biosynthesis and serotonergic synapses were enriched in LMCI/Control. In LMCI/EMCI, multiple amino acid metabolism and antibiotic synthesis were found (Fig. 3I-K). These metabolites may potentially contribute to the progression of MCI through altered pathways.

Characteristics of m6A methylated mRNAs

The differential expression patterns of regulatory factors of m6A among EMCI and LMCI with healthy control individuals were detected, including writers (METTL3 and METTL4) and erasers (FTO and ALKBH5) (Fig. 4). As the results showed, in the EMCI group, upregulated METTL3 ($P = 0.005$) but downregulated METTL4 ($P = 0.038$) were observed. Besides, there was a decreased trend of METTL4 in the LMCI group than Control group ($P = 0.071$). Down-regulated ALKBH5 was measured in EMCI and LMCI groups ($P < 0.001$) while no difference was found in FTO mRNA expression. Above all, disturbed m6A methylation in mRNAs may be attributed to the dynamic changes of writers and erasers.

To clarify the specific alterations of m6A transcripts in the peripheral blood of individuals with different cognitive levels, the m6A mRNA Epitranscriptomic Microarray ($n = 4$/group) was carried out, probing 42,508 mRNAs. By labeling differentially methylated mRNAs with Cy5 fluorescent dye, microarray profiling revealed that there were 21,756, 21,624, and 7,557 differentially methylated mRNA transcripts in comparisons among EMCI/Control, LMCI/Control, and LMCI/EMCI, respectively (fold change ≥ 1.5 or ≤ 0.7; $P < 0.05$). Specifically, 7,065 hypermethylated mRNAs and 14,691 hypomethylated mRNAs were found in EMCI/Control. In similar cases, there were 7,104 hypermethylated mRNAs and 14,520 hypomethylated mRNAs in LMCI/Control. These results suggested that there may be similar methylation patterns in the EMCI and LMCI groups when compared with the Control group. Whereas in the LMCI/EMCI comparison, the number of differentially methylated genes decreased remarkably, in which 2,569 mRNAs were hypermethylated and 4,988 mRNAs were hypomethylated. The hierarchical clustering heatmap determined the interaction between samples and classified them according to the similarity of m6A methylation level (Fig. 5A-C). As the data suggested, hypomethylation was the major m6A modification mode in different comparison schemes (EMCI/Control: 67.5%; LMCI/Control: 67.1%; LMCI/EMCI: 66.0%).

Furthermore, the total mRNAs were labeled with Cy3 fluorescent dye to compare the differential expression patterns of mRNAs in microarray. As shown in the volcano map (Fig. 5D-F), a total of 5,369 mRNAs were differentially expressed in EMCI/Control (3364 were upregulated and 2005 downregulated). When LMCI was compared with the Control group, as many as 15,922 differentially expressed genes were detected, including 8,912 upregulated mRNAs and 7,010 downregulated mRNAs. This number was 12,250 in LMCI/EMCI (6907 regulated and 5343 downregulated). (fold change ≥ 1.5 or ≤ 0.7, $P < 0.05$).

The intersection of differential methylation and differentially expressed mRNAs was presented by the four-quadrant diagram in Fig. 5G-I. The results showed that hypermethylated mRNAs with up-regulated expression (Hyper-Up) and hypomethylated mRNAs with down-regulated expression (Hypo-Down) accounted for the

largest proportion of altered mRNAs. Notably, in EMCI/Control and LMCI/Control, there were no hypermethylated downregulated (Hyper-Down) mRNAs and only a few hypomethylated upregulated (Hypo-Up) mRNAs. Similarly, in the comparison of LMCI/EMCI, only 3.45% and 3.49% of mRNAs were Hyper-Down and Hypo-Up, while the proportions of Hyper-Up and Hypo-Down were 40.59% and 52.47% respectively. These results indicated that hypermethylation was accompanied by upregulation of mRNAs expression, whereas hypomethylation was associated with downregulation.

On the basis of the above correlation analysis, we further analyzed the intersection of mRNAs with common changes as well as the specific alteration in each comparison, which was shown in the form of Venn diagrams (Fig. 5J-L). In detail, a total of 487 mRNAs were Hyper-Up while 341 mRNAs were Hypo-Down, but no mRNA was Hyper-Down or Hypo-Up in all three groups. It is worth noting that the intersection of LMCI/EMCI and EMCI/Control had no common altered mRNAs in any of the four interaction patterns, intimating that the LMCI group exhibited more divergent methylation and gene expression patterns compared to the Control group.

GO analysis was conducted to scan potential gene functions associated with differentially methylated mRNAs. The top 10 GO items of hypermethylation and hypomethylation in pairwise comparison were presented in Fig. 6A-F. Briefly, in EMCI/Control and LMCI/Control, hypermethylated mRNAs were widely distributed in the nucleus, organelles, and cytosol, along with participating in the regulation of RNA biosynthetic and metabolic processes by binding nucleic acid and DNA components. Similarly, in LMCI/EMCI, hypermethylated mRNAs were involved in regulating nitrogen compound metabolic process and cellular components through binding proteins and transcription factors, with the location of organelles and cytoplasm. Among the hypomethylated mRNAs, EMCI/Control and LMCI/Control were distributed in organelles and cytosol. The former was involved in protein transport and protein metabolism by binding proteins and lipids. The latter was bound to a variety of functional proteins involved in phosphorus metabolism and localization. Notably, the hypomethylated mRNAs in LMCI/EMCI were widely distributed in neurons, synapses, and cell junctions, which were involved in organ development and signal transduction processes such as the nervous system through ion channels and enzymes.

To explore the possible molecular pathways of differentially methylated mRNAs, KEGG analysis was carried out. The top 10 enriched pathways were shown in Fig. 7A-F. Among the hypermethylated mRNAs, 123, 139, and 74 pathways were enriched in EMCI/Control, LMCI/Control, and LMCI/EMCI, respectively. The first two were mainly related to pathogen infection, lipids, and atherosclerosis, while the last one was involved in pathways such as bacterial infection, choline metabolism in cancer, and platelet activation. However, relatively few pathways were enriched in the hypomethylated mRNAs. But remarkably, key pathways of AD and cholesterol metabolism have been found in 52 pathways of EMCI/Control and 45 pathways of LMCI/Control (Fig. 8), as well as Parkinson's disease and Huntington's disease. These results recommended that hypomethylated mRNAs may be involved in the development of neurodegenerative diseases such as AD, Parkinson's disease, and Huntington's disease, in which the related signal molecules may be crucial targets for further exploration and intervention of cognitive dysfunction.

Prediction of oxysterols, gut metabolites, and m6A in EMCI and LMCI individuals

To investigate the roles of oxysterols, gut metabolites, and their combination on the risk of different stages of MCI, logistic regression analysis and receiver operating characteristics (ROC) were conducted. As shown in Tables 5, 27-OHC was associated with increased risk of EMCI (OR: 1.272; 95% CI: 1.056, 1.532) and LMCI (OR: 1.364; 95% CI: 1.119, 1.663), so was 24S-OHC (EMCI, OR: 1.132; 95% CI: 1.029, 1.245; LMCI, OR = 1.145; 95% CI: 1.038, 1.264). Notably, the area under curve (AUC) indicated that the combination of 27-OHC with 24S-OHC performed better than either one of the two in both EMCI (27-OHC: 0.630; 24S-OHC: 0.696; 27-OHC + 24S-OHC: 0.729) and LMCI (27-OHC: 0.707; 24S-OHC: 0.697; 27-OHC + 24S-OHC: 0.774) (Fig. 9A-C).

Further, 10 typical gut metabolites whose relative levels differed among groups were also analyzed in relation to the diagnosis of MCI (Fig. 9D-F). When comparing EMCI with Control, Fasciculic acid B (OR: 0.404; 95% CI: 0.195, 0.837; AUC: 0.700), Phorbol myristate (OR: 0.306; 95% CI: 0.114, 0.817; AUC: 0.692), 2,3-dinor, 6-keto-pgf1alpha (OR: 0.371; 95% CI: 0.144, 0.955; AUC: 0.622) could be considered protective factors for the occurrence of EMCI. Whereas, elevated Biochanin a 8-c-glucoside (OR: 7.640; 95% CI: 1.792, 32.573; AUC: 0.723), Procyanidin dimer B7 (OR: 2.877; 95% CI: 1.117, 7.409; AUC: 0.664), Thymol-beta-d-glucoside (OR: 2.967; 95% CI: 1.052, 8.363; AUC: 0.637), and N2-Fructopyranosylarginine (OR: 4.138; 95% CI: 1.147, 14.934; AUC: 0.664) were risk factors for the occurrence of LMCI. Interestingly, all 10 gut metabolites could be used to differentiate between EMCI and LMCI (Table 6). The diagnostic checks for the regression models of oxysterols and gut metabolites were presented in Figure S1 and Table S7-S8.

The correlation analysis of oxysterols and gut metabolites was conducted, as presented in Fig. 9G, negative correlation was found between 24S-OHC and N2-Fructopyranosylarginine (r = -0.281, P = 0.018). Besides,

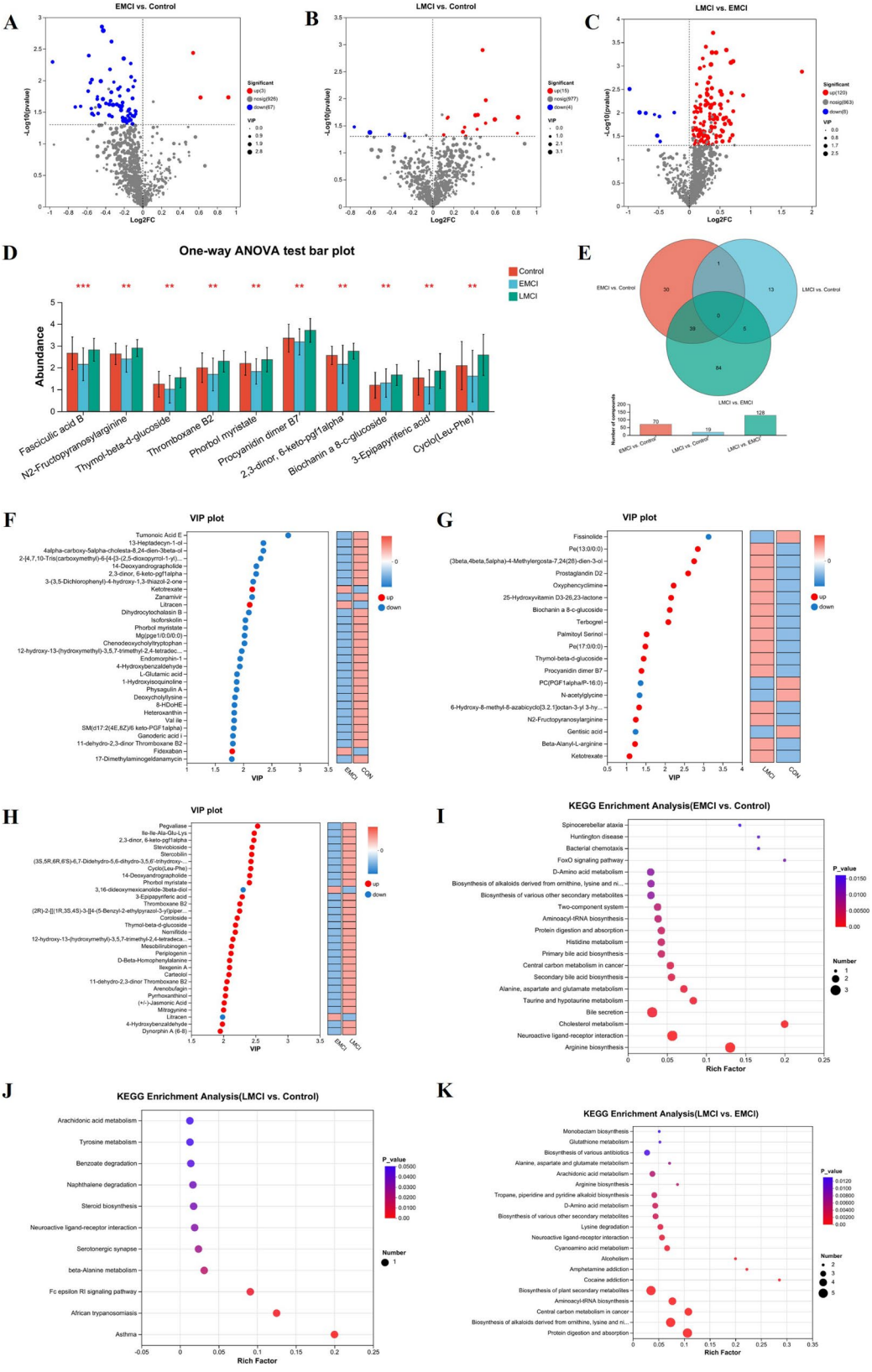

Fig. 3 (See legend on next page.)

(See figure on previous page.)

Fig. 3 Differential metabolites and metabolomics analysis. **A-C**: Volcano diagrams analysis of differential metabolites in EMCI/Control (**A**), LMCI/Control (**B**), and LMCI/EMCI (**C**). **D**: Multi-groups comparative analysis. The y-axis represented the names of metabolites, and the x-axis represented the average relative abundance of metabolites in different groups. **E**: Venn diagram of differential metabolisms in pairwise comparison, the number of overlapping parts represented the amounts of metabolites shared by multiple control groups, and the number of non-overlapping parts represented the amounts of metabolites unique to the corresponding groups. **F-H**: VIP diagrams were used to rank the differential contribution of metabolites to EMCI/Control (**F**), LMCI/Control (**G**), and LMCI/EMCI (**H**). The y-axis was the name of the metabolites, and the x-axis was the VIP value corresponding to the metabolites. The left and right color blocks on the right represented corresponding groups. Red and blue represented the high and low expression level of the metabolites in the group, respectively. **I-K**: KEGG pathway analyses of differential metabolites in EMCI vs. Control (**I**), LMCI vs. Control (**J**), and LMCI vs. EMCI (**K**)

the above meaningful gut metabolites combined with 27-OHC and 24S-OHC were added to different models together to differentiate between EMCI and LMCI, and the results were shown in Fig. 9H-J. The AUC of combined 27-OHC and 24S-OHC with Fasciculic acid B, Phorbol myristate, and 2,3-dinor, 6-keto-pgf1alpha when diagnosed with EMCI was 0.877 (sensitivity: 0.727, specificity: 0.857) while the 4 gut metabolites with 27-OHC and 24S-OHC had a combined AUC of 0.952 (sensitivity: 0.84, specificity: 0.952). In distinguishing between EMCI and LMCI, the AUC of the top 3 gut metabolites (Procyanidin dimer B7, Thromboxane B2, and 2,3-dinor, 6-keto-pgf1alpha) combined with 27-OHC and 24S-OHC was 0.765, which was lower than the combination without oxysterols (AUC = 0.813). It suggested that the combination of oxysterols with gut metabolites were considerable biomarkers to be taken into account for distinguishing different stages of cognitive impairment from healthy controls.

Besides, heatmaps were used to evaluate the correlation between gut metabolites and differentially m6A-methylated mRNAs. Among the hypermethylated and up-regulated mRNAs (Fig. 10A), negative correlations were found between Phorbol myristate with SMC3 (r = -0.622, P = 0.031) and JAKMIP2 (r = -0.615, P = 0.033). Whereas, among the hypomethylated and down-regulated mRNAs (Fig. 10B), positive correlations were discovered between Phorbol myristate with CACNA1G (r = 0.713, P = 0.009), CSF3 (r = 0.650, P = 0.022), and QPRT (r = 0.622, P = 0.031). The results suggested that Phorbol myristate may be a key metabolite very closely related to aberrant m6A modifications.

To deeply explore the possible association of gut metabolites with differentially m6A methylated transcripts, their enriched KEGG metabolic pathways were compared. A total of 34 metabolic pathways were shared between gut metabolites and m6A methylation, in which the metabolism of various substances such as cholesterol, various amino acids, and nucleotides were included. Through various organismal systems such as dopaminergic synapse and serotonergic synapse, a variety of neurodegenerative diseases like Parkinson's disease and Huntington's disease were enriched, indicating that the altered gut metabolites may participate in the dynamic modification of m6A through a shared metabolic pathway, which may be the essential processes of oxysterols-induced cognitive impairment (Table 7).

Discussion

In this study, we explored the changes in oxysterols, gut metabolites, and m6A methylation, as well as their correlations in different stages of MCI. Our study confirmed that LMCI had worse performance than EMCI in almost all cognitive assessments and was accompanied by elevated serum oxysterols and Aβ. Furthermore, the alterations of gut metabolites and m6A methylation in EMCI and LMCI groups were described in detail. Representative gut metabolites not only presented better ability to distinguish EMCI and LMCI combined with 27-OHC and 24S-OHC, but also shared multiple KEGG-enriched pathways with m6A methylation for cholesterol metabolism and neurodegenerative diseases.

According to the severity of MCI, MCI is divided into EMCI and LMCI. LMCI is recognized as the transition stage between the post-MCI state and the pre-AD state, with more cognitive domain dysfunction and a higher AD conversion rate [25–27]. Although EMCI and LMCI are distinguished only by the delayed recall test of LMT (WMS-R) and education years, LMCI subjects perform worse than EMCI in several tests of global and multi-dimensional cognitive function in our study, including MoCA, AVLT, SDMT, LMT, DSF, and SCWT, indicating that LMCI individuals are not only impaired by delayed memory in LMT but also damaged in verbal function, processing speed, executive function, working memory and so on. Lin *et al.* have certified that the LMCI group not only performed worse than EMCI in serious multi-dimensional cognitive function tests but also declined faster annually in these tests [27]. Another 6-year longitudinal study also confirmed that the LMCI group had the highest risk of transforming into AD, and EMCI also remained an at-risk situation [26]. It is indicated that pre-AD risk conditions should be expanded from LMCI to EMCI.

Aβ deposition is recognized as the driving factor of the pathological process of AD [28]. It is produced by the sequential cleavage of APP by BACE1. Our previous study has confirmed that the serum Aβ level is increased in the MCI group [5], but few studies have extended the changes of serum Aβ concentration to the EMCI and LMCI stages. It was demonstrated in our results that

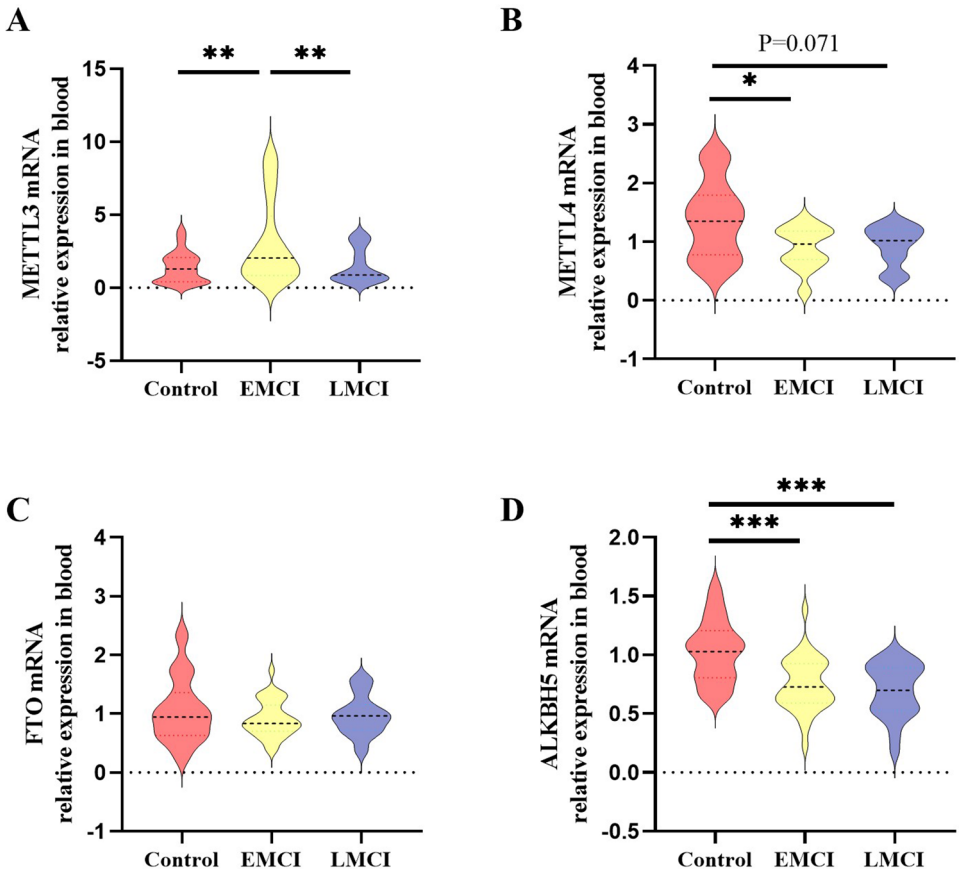

Fig. 4 The expression of m6A regulators. METTL3 (**A**), METTL4 (**B**), FTO (**C**), and ALKBH5 (**D**) were analyzed by ANOVA test. *$P < 0.05$, **$P < 0.01$. Abbreviations: EMCI, early mild cognitive impairment; LMCI, late mild cognitive impairment; METTL3, methyltransferase-like 3; METTL4, methyltransferase-like 4; FTO, fat mass and obesity-associated; ALKBH5, AlkB homolog 5

serum Aβ level was evidently increased in the LMCI group, while the Control and EMCI groups presented similar concentrations, implying that during the progression of MCI, the rise of Aβ serum concentrations may occur in the late stage. In addition, the mRNA expression of APP in the EMCI group was notably reduced compared with the Control group but tended to rise again in the LMCI group, which was inconsistent with Ramasamy *et al.*'s conclusion that serum APP levels increased in MCI and AD patients [29]. However, given that their study did not further group MCI patients, whether the level of APP fluctuates in the process from normal cognition to EMCI and LMCI should be evaluated by repeated experiments with more samples.

As the main oxidative metabolite of cholesterol in the peripheral circulation, 27-OHC initially played an important role in the growth and metastasis of breast cancer acting as estrogen receptor and liver X receptor (LXR) ligand [30]. Due to the property that 27-OHC can freely cross the blood-brain barrier (BBB), its potential function in cognition-related diseases such as AD has gradually attracted attention. Our published works have reported 27-OHC as an independent risk factor for MCI [31], which promotes Aβ accumulation through various mechanisms such as immune imbalance [4] and gut-brain axis [10]. Oxysterols including 27-OHC are also quantified in ox-LDL, which is a new complex formed after oxidation modification of native LDL [32]. Ox-LDL is a prominent biomarker of cardiovascular disease because of its strong ability to promote oxidative stress [33]. The clearance of ox-LDL could be inhibited by Aβ, which led to the extracellular accumulation of ox-LDL and the perpetuation of lipid peroxidation [34]. However, whether ox-LDL is a differential metabolite in cognition has not been concluded [35, 36]. Compared with diabetes patients without MCI, the increased serum ox-LDL in diabetes patients with MCI suggested that ox-LDL may be a promoter in the development of MCI [37]. Above all, as derivative metabolites of cholesterol, disturbed oxysterols, and ox-LDL, their role in accelerating the progression of MCI should be made a point.

Alteration of gut metabolites in AD has been reported in several studies [38], but few studies have investigated the changes in gut metabolites in the MCI stage. Gao *et al.* found that fecal SCFAs were reduced in MCI patients and negatively correlated with Aβ deposition

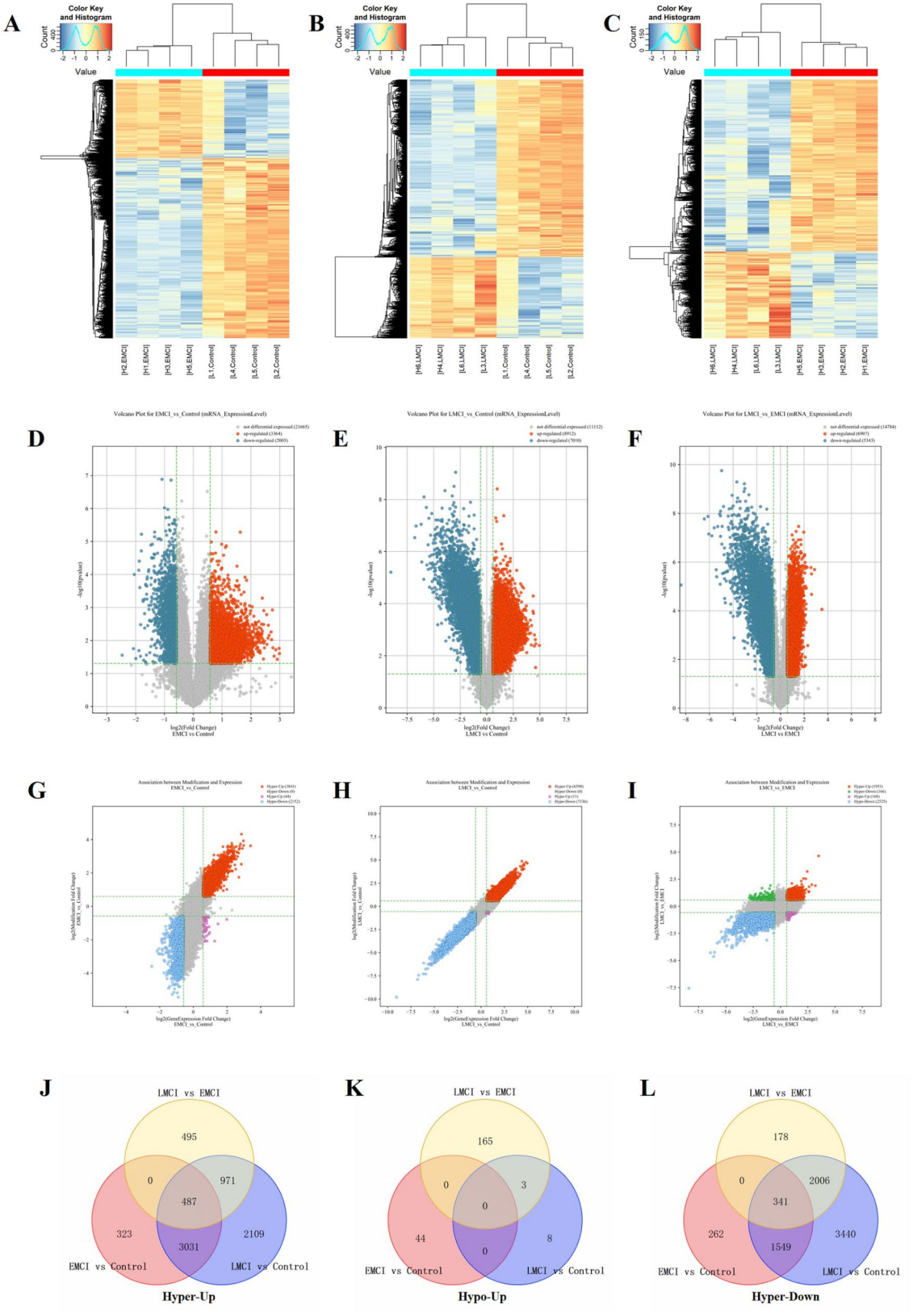

Fig. 5 (See legend on next page.)

(See figure on previous page.)

Fig. 5 m6A mRNA Epitranscriptomic Microarray analysis. **A-C**: Hierarchical clustering heatmap of EMCI/Control (**A**), LMCI/Control (**B**), and LMCI/EMCI (**C**). Each row represented one mRNA, and each column represented one sample. **D-F**: Volcano plot analysis of EMCI/Control (**D**), LMCI/Control (**E**), and LMCI/EMCI (**F**). Red boxes represented upregulated transcripts (≥ 1.5-fold change, $P < 0.05$), and blue boxes represented downregulated transcripts (≤ 0.7-fold change, $P < 0.05$). **G-I**: Four-quadrant diagram of changed transcripts in both m6A methylation and mRNA expression of EMCI/Control (**G**), LMCI/Control (**H**), and LMCI/EMCI (**I**). Red dots: hypermethylated-upregulated mRNAs; green dots: hypermethylated-downregulated mRNAs; purple dots: hypomethylated-upregulated mRNAs; blue dots: hypomethylated-downregulated mRNAs. $P < 0.05$. **J-L**: The interaction between m6A methylation and mRNA expression. (**J**) Hypermethylation-upregulation, (**K**) Hypomethylation-upregulation, (**L**) Hypomethylation-downregulation

in brain regions [39], while the specific changes in gut metabolite profiles in different stages of MCI have not been expounded. Our study found that most metabolites showed a common feature of a decrease in the EMCI group, and the LMCI group exhibited a relatively close profile to the Control group. Besides, metabolite traceability analysis of gut metabolites showed that almost half of the gut metabolites did not belong to the host or gut microorganisms, of which the possible sources may include food, plant extracts, herbal medicines as well as drugs [40–43]. Thus, metabolite abnormalities disturbed by exogenous pathways may be an important factor in the development of MCI. As reported in our previous study, the changes in gut metabolites could be attributed to disordered oxysterols, especially 27-OHC [10]. The correlation and ROC curve suggested that serum 27-OHC and 24S-OHC can be used as the diagnostic basis of EMCI and LMCI to distinguish Control combined with key gut metabolites. Although no significant differences in 27-CA levels were observed in the overall comparison, subgroup analysis revealed that the EMCI group exhibited lower concentrations of 27-CA compared to the Control group within the specific subset of gut microbial metabolites. Notably, given that gut metabolites demonstrated significant correlation solely with 24S-OHC, these observations introduce complexity in interpreting the interplay between oxysterols and gut metabolites. However, as 27-CA constitutes a critical metabolic derivative of 27-OHC, its concentration dynamics serve as an indirect indicator of the imbalance between oxysterols 27-OHC and 24S-OHC. Furthermore, these observations indicate that the association between oxysterols and gut metabolites likely arises from coordinated variations involving both 27-OHC (and its downstream metabolites) and 24S-OHC, rather than isolated perturbations in a single molecular entity. Besides, given that gut microbiota-derived metabolites are susceptible to environmental influences, the gut metabolites identified in our study may not represent optimal biomarkers. Subsequent studies employing targeted metabolomics or animal intervention experiments are warranted to elucidate key metabolites mechanistically involved in cognitive function modulation.

Although abnormal m6A modification has been confirmed to be a vital epigenetic mark in AD pathogenesis, few studies have turned their attention forward to the MCI stage. Du *et al*. found that m6A regulators SNRPG and SNRPD2 can be used as potential biomarkers to predict the conversion of MCI to AD [14]. However, the m6A modification enzymes and abnormal methylated mRNA transcripts profile in MCI individuals have not been comprehensively displayed. METTL4 is a newly identified m6A methyltransferase [44, 45]. Our study found that the mRNA expression of METTL4 was reduced in the MCI groups. Building upon prior evidence that 27-OHC impairs memory via suppression of m6A methylation [13], whether this effect is mediated through METTL4-dependent regulation of the m6A epitranscriptomic landscape warrants further investigation. Future studies should employ METTL4-knockout models or selective m6A modulators to dissect this pathway. By comparing the differentially methylated mRNAs, it was found that the methylation patterns of EMCI and LMCI were closer, in which hypomethylated and downregulated mRNAs accounted for the majority, suggesting that abnormal decreased methylation of m6A occurred in the early stage of MCI.

The cognitive impairment caused by oxysterols may be the result of the combined action of gut metabolites and m6A. A few studies have demonstrated the regulatory effect of gut metabolite alterations on the m6A epitranscriptome landscape. Through fecal microbiota transplantation, Yang *et al*. demonstrated that abnormal bile acid metabolism drastically shifted the m6A methylation in different tissues, proving a direct connection between gut metabolites and m6A biology [17]. Besides, another gut metabolite, trimethylamine N-oxide (TMAO) has been found to increase the level of m6A and the proinflammatory state [46]. One of the mechanisms by which TMAO promotes inflammation is inhibiting the expression of the demethylase FTO and the reader protein IGF2BP2, leading to a decrease in the m6A level and activation of NLRP3 in the microglia, which ultimately exacerbated the neurological damage in ischaemic stroke [47]. Butyric acid, a common SCFA, is one of the classical products of gut metabolites. It has been demonstrated that butyric acid treatment can directly suppress the expression of METTL3, leading to a reduction in the methylation level and mRNA expression of its downstream target, FOSL2, which contributes to the improvement of the inflammatory milieu in polycystic ovary syndrome [48]. However, no article has yet identified a biological function of the 10 kinds of gut metabolites with oxysterols or RNA methylation, possibly because

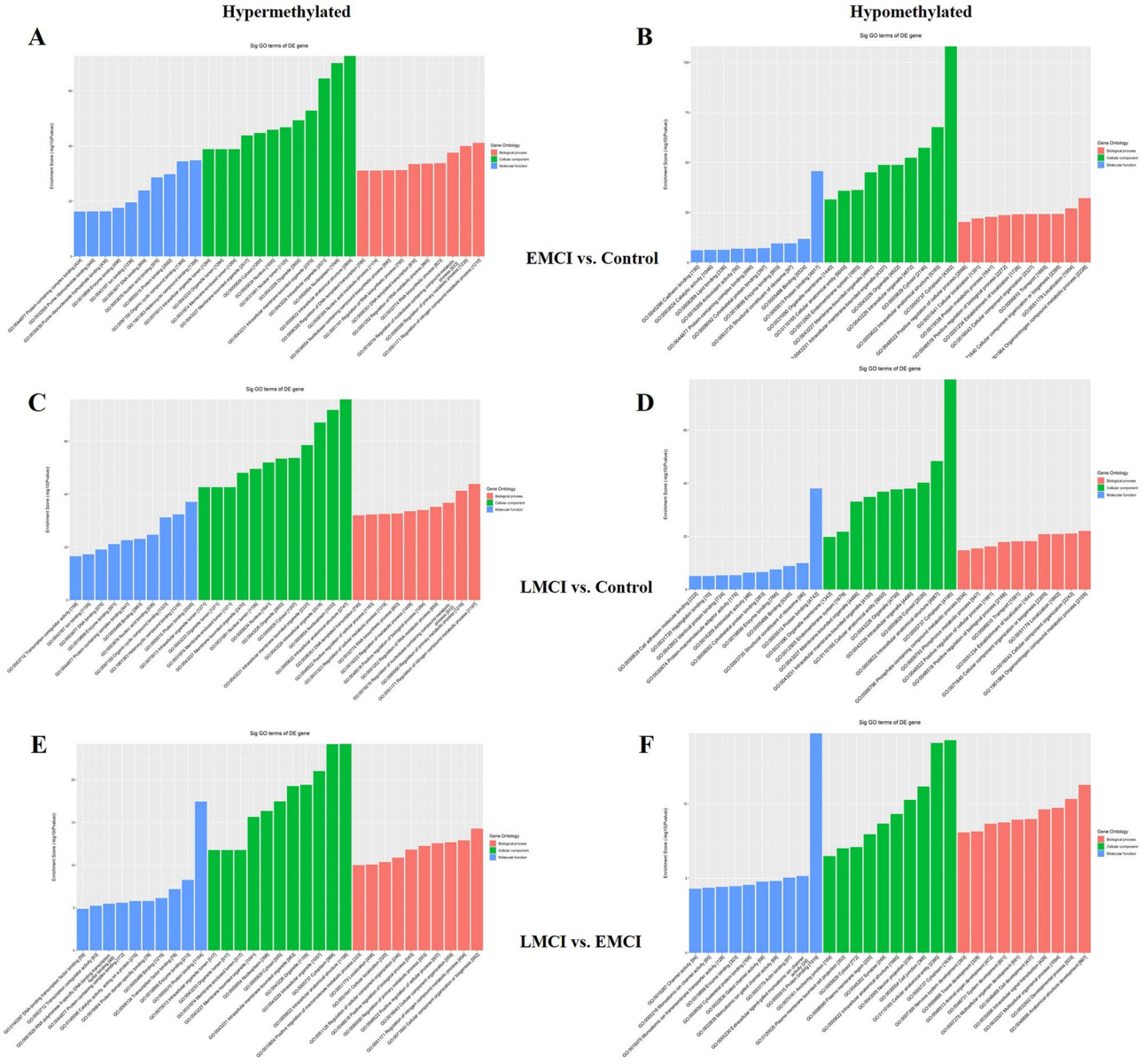

Fig. 6 Gene Ontology of differentially methylated mRNAs. (**A**), (**C**), (**E**) presented the top ten enriched GO items of differentially hypermethylated mRNAs among EMCI/Control (**A**), LMCI/Control (**C**), and LMCI/EMCI (**E**). (**B**), (**D**), (**F**) presented the top ten enriched GO items of differentially hypomethylated mRNAs among EMCI/Control (**B**), LMCI/Control (**D**), and LMCI/EMCI (**F**)

these gut metabolites are not common species, so there are fewer studies on them, and the cascade pathways and biological functions of these metabolites in combination with RNA methylation could be explored subsequently using animal studies. Our study found that the combination of gut metabolites and 27-OHC and 24S-OHC presented a better ability to distinguish EMCI and LMCI from Control. Furthermore, a comparison of KEGG-enriched pathways for differential gut metabolites and m6A methylation revealed 34 shared pathways, including cholesterol metabolism and multiple neurodegenerative diseases, indicating that the possibility of gut metabolites as potential bridges to oxysterol and m6A methylated mRNAs could be considered. In the future, to enable the use of oxysterols and gut metabolites as biomarkers for exploring the development of MCI, it is necessary to validate the current study in a larger prospective cohort of multiple populations. In addition, in *vivo* or in *vitro* biological experiments using combined interventions of oxysterols and specific gut metabolites are necessary to determine their biological effects and potential mechanisms on animal or cellular models of AD.

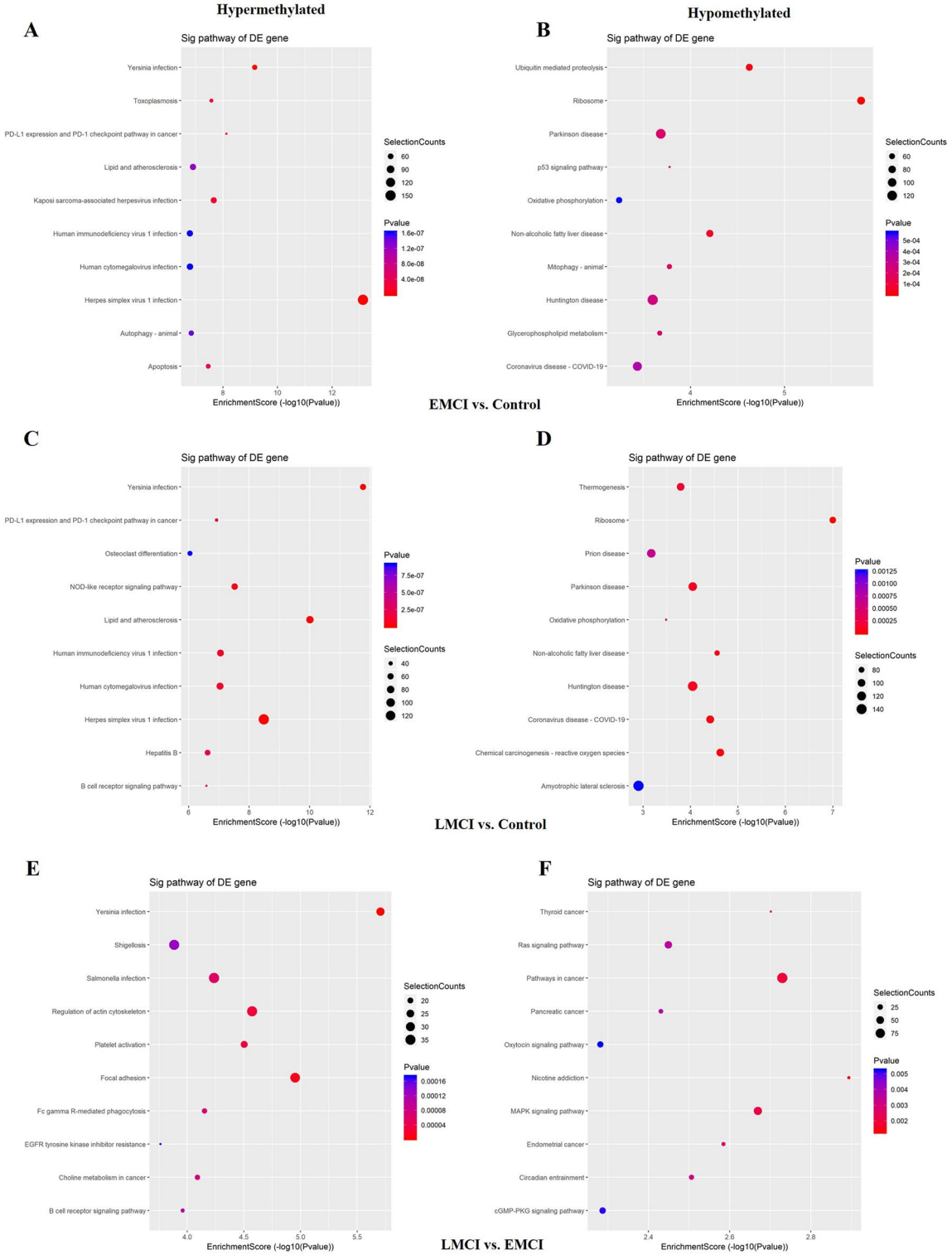

Fig. 7 KEGG pathway analyses of differentially methylated mRNAs. (**A**), (**C**), (**E**) presented the top ten enriched pathways of differentially hypermethylated mRNAs among EMCI/Control (**A**), LMCI/Control (**C**), and LMCI/EMCI (**E**). (**B**), (**D**), (**F**) presented the top ten enriched pathways of differentially hypomethylated mRNAs among EMCI/Control (**B**), LMCI/Control (**D**), and LMCI/EMCI (**F**)

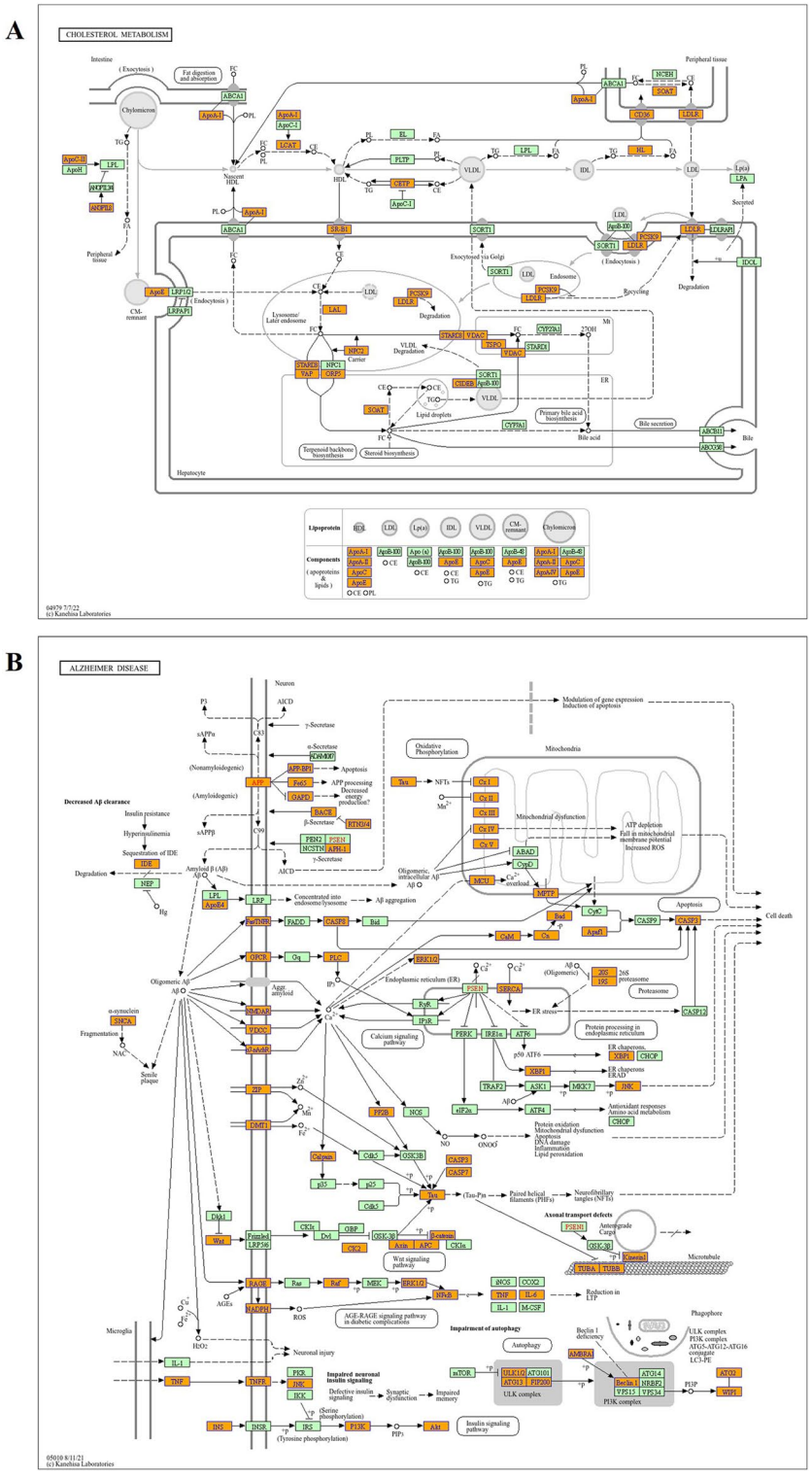

Fig. 8 Schematic overviews of signaling pathways of enriched hypomethylated mRNAs in LMCI/Control. **A**: Cholesterol metabolism. **B**: Alzheimer's disease. Orange nodes: hypomethylated mRNAs; Green nodes: other mRNAs without m6A methylation in the pathway

Table 5 Associations of oxysterols with risks of EMCI and LMCI

	EMCI/CON		LMCI/CON		LMCI/EMCI	
Oxysterols	**OR**	***P***	**OR**	***P***	**OR**	***P***
27-OHC	1.272 (1.056, 1.532)	0.011*	1.364 (1.119, 1.663)	0.002*	1.066 (0.913, 1.245)	0.417
24S-OHC	1.132 (1.029, 1.245)	0.011*	1.145 (1.038, 1.264)	0.007*	1.003 (0.921, 1.092)	0.948
27-CA	0.967 (0.931, 1.003)	0.074	0.994 (0.963, 1.026)	0.719	1.023 (0.989, 1.059)	0.182
7-HOCA	1.009 (0.980, 1.038)	0.563	0.999 (0.967, 1.031)	0.929	0.987 (0.953, 1.021)	0.442

Abbreviations: EMCI, early mild cognitive impairment; LMCI, late mild cognitive impairment; OR, odds ratio; 27-OHC, 27-hydroxycholesterol; 24S-OHC, 24S-hydroxycholesterol; 27-CA, 3β-hydroxy-5-cholestenoic acid; 7-HOCA, 7α-hydroxy-3-oxo-4-cholestenoic acid. ∗ $P < 0.05$

Limitations

Due to the cost constraints of m6A methylation detection, it was not possible to perform m6A epitranscriptome on a large number of samples, and therefore regression analysis related to cognition could not be conducted by differentially methylated mRNAs. Furthermore, the correlation analysis between differentially methylated mRNAs and gut metabolites provides preliminary evidence suggesting a potential association between phorbol myristate and m6A differential methylation. However, whether phorbol myristate functions as a critical gut metabolite inducing differential methylation, as well as the mechanistic linkage between m6A methylation and cognitive impairment, requires direct validation through systematic animal intervention studies. Besides, the individuals included in this study were made up of Chinese, which better represents the true status of Chinese older adults, but limits the generalizability of the findings to other populations around the world to some extent, and more in-depth exploration in global cohorts with multiple populations could be considered in the future.

Conclusion

This study demonstrated that disordered oxysterols, gut metabolites, and m6A methylation were correlated with different stages of MCI. Gut metabolites may be the potential link between oxysterols and m6A epitranscriptome in the progress of cognitive impairment.

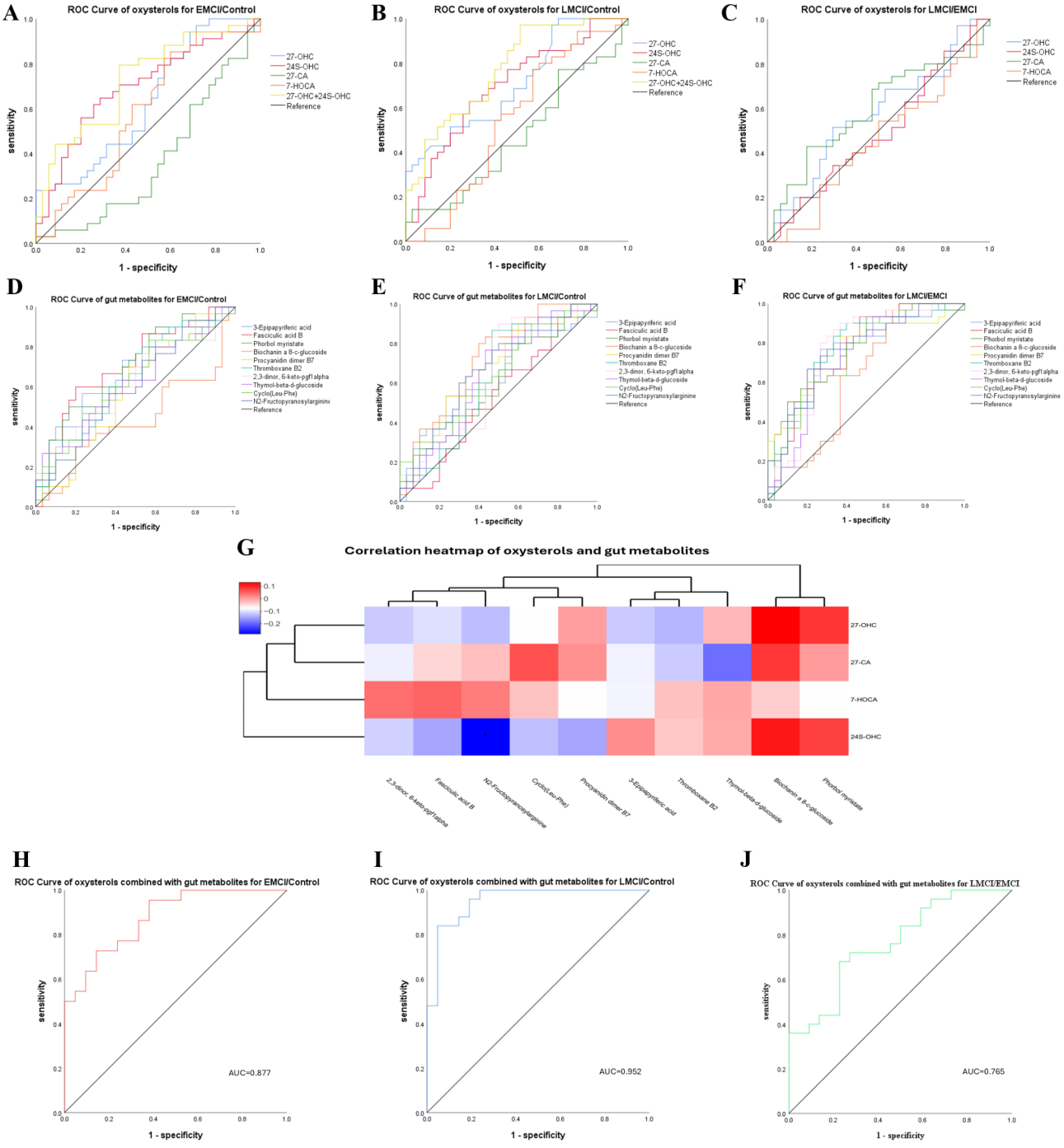

Fig. 9 ROC curve of oxysterols (**A-C**), gut metabolites (**D-F**), and the combination of oxysterols and gut metabolites (**H-J**), and the correlation heatmap of oxysterols and metabolites (**G**)

Table 6 Associations of gut metabolites with risks of EMCI and LMCI

	EMCI/CON		LMCI/CON		LMCI/EMCI	
Gut metabolites	**OR**	***P***	**OR**	***P***	**OR**	***P***
3-Epipapyriferic acid	0.510 (0.255, 1.018)	0.056	1.681 (0.864, 3.271)	0.126	3.024 (1.495, 6.117)	0.002*
Fasciculic acid B	0.404 (0.195, 0.837)	0.015*	1.455 (0.648, 3.266)	0.363	4.721 (1.863, 11.965)	0.001*
Phorbol myristate	0.306 (0.114, 0.817)	0.018*	1.815 (0.688, 4.785)	0.228	5.341 (1.844, 15.470)	0.002*
Biochanin a 8-c-glucoside	1.329 (0.578, 3.053)	0.503	7.640 (1.792, 32.573)	0.006*	3.472 (1.165, 10.347)	0.025*
Procyanidin dimer B7	0.630 (0.268, 1.477)	0.288	2.877 (1.117, 7.409)	0.029*	5.739 (1.843, 17.867)	0.003*
Thromboxane B2	0.544 (0.257, 1.152)	0.112	2.523 (0.934, 6.816)	0.068	5.487 (1.738, 17.326)	0.004*
2,3-dinor, 6-keto-pgf1alpha	0.371 (0.144, 0.955)	0.040*	4.057 (0.896, 18.369)	0.069	7.101 (1.662, 30.337)	0.008*
Thymol-beta-d-glucoside	0.528 (0.224, 1.243)	0.144	2.967 (1.052, 8.363)	0.040*	5.458 (1.890, 15.759)	0.002*
Cyclo(Leu-Phe)	0.692 (0.439, 1.090)	0.112	1.613 (0.955, 2.723)	0.074	2.281 (1.339, 3.886)	0.002*
N2-Fructopyranosylarginine	0.453 (0.170, 1.211)	0.115	4.138 (1.147, 14.934)	0.030*	8.819 (2.133, 36.459)	0.003*

Abbreviations: EMCI, early mild cognitive impairment; LMCI, late mild cognitive impairment; OR, odds ratio. $* P < 0.05$

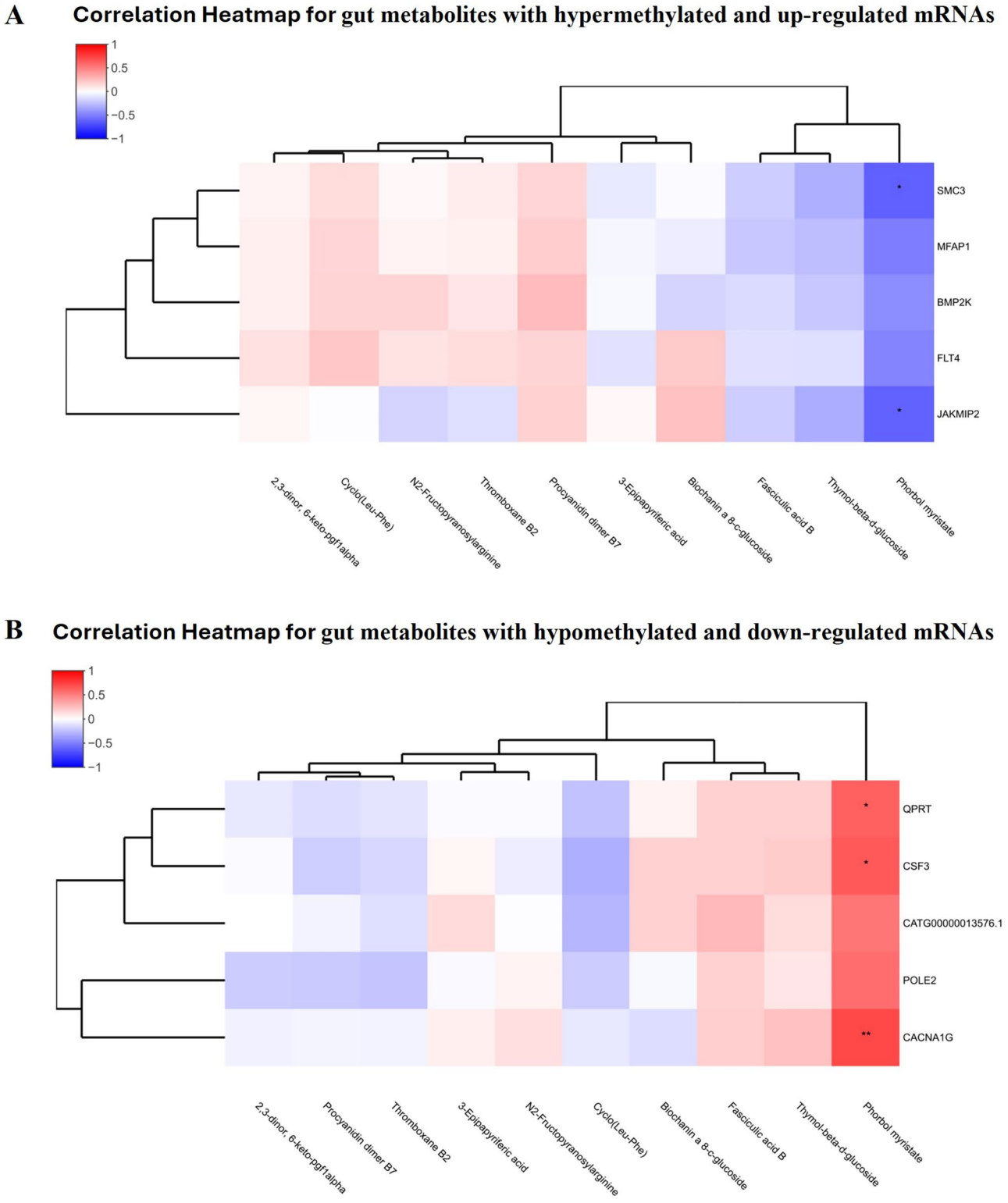

Fig. 10 Heatmaps of the correlation between gut metabolites and hypermethylated and up-regulated mRNAs (**A**), and hypomethylated and down-regulated mRNAs (**B**). *$P < 0.05$, **$P < 0.01$

Table 7 Common KEGG pathways in gut metabolites and m6A related to cholesterol and cognition

First Category	Second Category	Pathway Description	Pathway ID
Human Diseases	Neurodegenerative disease	Spinocerebellar ataxia	map05017
		Parkinson disease	map05012
		Huntington disease	map05016
		Amyotrophic lateral sclerosis	map05014
	Infectious disease: bacterial	Shigellosis	map05131
		Tuberculosis	map05152
	Infectious disease: parasitic	African trypanosomiasis	map05143
Metabolism	Lipid metabolism	Glycerophospholipid metabolism	map00564
	Amino acid metabolism	Valine, leucine and isoleucine biosynthesis	map00290
		Cysteine and methionine metabolism	map00270
		Lysine degradation	map00310
	Carbohydrate metabolism	Glyoxylate and dicarboxylate metabolism	map00630
	Metabolism of other amino acids	Glutathione metabolism	map00480
	Nucleotide metabolism	Purine metabolism	map00230
Organismal Systems	Nervous system	Dopaminergic synapse	map04728
		Serotonergic synapse	map04726
		Retrograde endocannabinoid signaling	map04723
		Long-term potentiation	map04720
	Digestive system	Cholesterol metabolism	map04979
		Mineral absorption	map04978
	Endocrine system	Melanogenesis	map04916
		Parathyroid hormone synthesis, secretion and action	map04928
		Prolactin signaling pathway	map04917
	Environmental adaptation	Circadian entrainment	map04713
	Immune system	Fc epsilon RI signaling pathway	map04664
Cellular Processes	Cell growth and death	Ferroptosis	map04216
Environmental Information Processing	Signal transduction	FoxO signaling pathway	map04068
		Phospholipase D signaling pathway	map04072
	Signaling molecules and interaction	Neuroactive ligand-receptor interaction	map04080

Abbreviations

24S-OHC	24S-hydroxycholesterol
27-CA	3β-hydroxy-5-cholestenoic acid
27-OHC	27-hydroxycholesterol
7-HOCA	7α-hydroxy-3-oxo-4-cholestenoic acid
AD	Alzheimer's disease
APP	Amyloid precursor protein
AUC	Area under curve
AVLT-IR	Auditory Verbal Learning Test-immediate recall
AVLT-LR	Auditory Verbal Learning Test-long recall
AVLT-SR	Auditory Verbal Learning Test-short recall
Aβ	Amyloid-β
BACE1	β-secretase
CHD	Coronary heart disease
DSB	Digit span backwards
DSF	Digit span forwards
EMCI	Early MCI
FC	Fold change
KEGG	Kyoto Encyclopedia of Genes and Genomes
LC-MS	Liquid chromatography-mass spectrometry
LDL-C	Low-density lipoprotein cholesterol
LMCI	Late MCI
LMT	Logical memory test
m6A	N6-methyladenosine
MCI	Mild cognitive impairment
METTL4	Methyltransferase-like 4
MMSE	Mini-Mental State Examination
MoCA	Montreal Cognitive Assessment
OPLS-DA	Orthogonal least partial squares discriminant analysis
ox-HDL	Oxidized HDL
ox-LDL	Oxidized LDL
PLS-DA	Partial Least squares-discriminant Analysis
RT-qPCR	Quantitative real-time PCR
ROC	Receiver operator characteristics
SCFAs	Short-chain fatty acids
SCWT-RIE	Stroop color-word test-reaction interfered effects
SCWT-TIE	Stroop color-word test-time interfered effects
TC	Total cholesterol
TMT-A	Trail making test-A
TMT-B	Trail making test-B
VIP	Variable Importance in Projection
WMS-R	Wechsler Memory Scale-recall

Supplementary Information

The online version contains supplementary material available at https://doi.org/10.1186/s13195-025-01743-5.

Supplementary Material 1

Acknowledgements
Not applicable.

Author contributions
Rong Xiao obtained the grants and designed the research. Wenjing Feng conducted experiments, analyzed the data and wrote the manuscript. Wenjing Feng, Mengwei Ju, Tao Wang, Kexin Yang, Shanshan Cui, Zhiting Guo, Miao Liu, JiaXuan Tao and Huiyan Yu collected the samples and conducted

face-to-face questionnaire. All authors have read and agreed to the published version of the manuscript.

Funding
This research was funded by the National Natural Science Foundation of China (Grand No. 82173501 and 82373557).

Data availability
The datasets used and/or analysed during the current study are available from the corresponding author on reasonable request.

Declarations

Ethics approval and consent to participate
The experiment was approved by the Ethics Committee of Capital Medical University (Z2023SY024) with signed informed consent from all individuals before each examination.

Consent for publication
Not applicable.

Competing interests
The authors declare no competing interests.

Author details
[1]School of Public Health, Capital Medical University, No.10 Xitoutiao, You An Men Wai, Beijing, China

Received: 14 December 2024 / Accepted: 15 April 2025
Published online: 13 May 2025

References

1. Gauthier S, Reisberg B, Fau - Zaudig M, Zaudig M, Fau - Petersen RC, Petersen Rc Fau -, Ritchie K, Ritchie K. Mild cognitive impairment. Lancet. 2006;367(9518):1262–70. Fau - Broich K, Broich K Fau - Belleville.
2. Aisen PS, Petersen Rc Fau -, Donohue MC, Donohue Mc Fau - Gamst A, Gamst A, Fau - Raman R, Raman R, Fau - Thomas RG, Walter S, et al. Clinical core of the Alzheimer's disease neuroimaging initiative: progress and plans. Alzheimers Dement. 2010;6(3):239–46.
3. Zhang J, Liu Q. Cholesterol metabolism and homeostasis in the brain. Protein Cell. 2015;6(4):254–64.
4. Wang T, Feng W, Ju M, Yu H, Guo Z, Sun X, Yang K, Liu M, Xiao R. 27-hydroxycholesterol causes cognitive deficits by disturbing Th17/Treg balance and the related immune responses in mild cognitive impairment patients and C57BL/6J mice. J Neuroinflammation. 2023;20(1):305.
5. Zhang X, Xi Y, Yu H, An Y, Wang Y, Tao L, Wang Y, Liu W, Wang T, Xiao R. 27-hydroxycholesterol promotes Aβ accumulation via altering Aβ metabolism in mild cognitive impairment patients and APP/PS1 mice. Brain Pathol. 2019;29(4):558–73.
6. Nguyen NM, Cho J, Lee CA-O. Gut microbiota and Alzheimer's disease: how to study and apply their relationship. Int J Mol Sci. 2023;24(4):4047.
7. Zhang X, Wang Y, Liu W, Wang T, Wang L, Hao L, Ju M, Xiao R. Diet quality, gut microbiota, and MicroRNAs associated with mild cognitive impairment in middle-aged and elderly Chinese population. Am J Clin Nutr. 2021;114(2):429–40.
8. Choi H, Mook-Jung I. Functional effects of gut microbiota-derived metabolites in Alzheimer's disease. Curr Opin Neurobiol. 2023;81:102730.
9. Zierer JA-O, Jackson MA-O, Kastenmüller G, Mangino MA-O, Long TA-O, Telenti A, et al. The fecal metabolome as a functional readout of the gut Microbiome. Nat Genet. 2018;50(6):790–5.
10. Wang Y, An Y, Ma W, Yu H, Lu Y, Zhang X, Wang Y, Liu W, Wang T, Xiao R. 27-Hydroxycholesterol contributes to cognitive deficits in APP/PS1 Transgenic mice through microbiota dysbiosis and intestinal barrier dysfunction. J Neuroinflammation. 2020;17(1):199.
11. Zhang R, Zhang Y, Guo F, Li S, Cui H. RNA N6-Methyladenosine modifications and its roles in Alzheimer's disease. Front Cell Neurosci. 2022;16:820378.
12. Meyer KD, Jaffrey SR. Rethinking m(6)A readers, writers, and erasers. Annu Rev Cell Dev Biol. 2017;33:319–42.
13. Sun X, Zhou C, Ju M, Feng W, Guo Z, Qi C, Yang K, Xiao R. Roseburia intestinalis supplementation could reverse the learning and memory impairment and m6A methylation modification decrease caused by 27-Hydroxycholesterol in mice. Nutrients. 2024;16(9):1288.
14. Du B, Zhang Y, Liang M, Du Z, Li H, Fan C, Zhang H, Jiang Y, Bi X. N6-methyladenosine (m6A) modification and its clinical relevance in cognitive dysfunctions. Aging. 2021;13(16):20716–37.
15. Xia L, Zhang F, Li Y, Mo Y, Zhang L, Li Q, et al. A new perspective on Alzheimer's disease: m6A modification. Front Genet. 2023;14:1166831.
16. Zhao F, Xu Y, Gao S, Qin L, Austria Q, Siedlak SL, et al. METTL3-dependent RNA m(6)A dysregulation contributes to neurodegeneration in Alzheimer's disease through aberrant cell cycle events. Mol Neurodegener. 2021;16(1):70.
17. Yang M, Zheng X, Fan J, Cheng W, Yan TM, Lai Y, et al. Antibiotic-Induced gut microbiota dysbiosis modulates host transcriptome and m(6)A epitranscriptome via bile acid metabolism. Adv Sci (Weinh). 2024;11(28):e2307981.
18. Zhu W, Si Y, Xu J, Lin Y, Wang JZ, Cao M, Sun S, Ding Q, Zhu LA-O, Wei JA-O. Methyltransferase like 3 promotes colorectal cancer proliferation by stabilizing CCNE1 mRNA in an m6A-dependent manner. J Cell Mol Med. 2020;24(6):3521–33.
19. Tao L, Liu K, Chen S, Yu H, An Y, Wang Y, Zhang X, Wang Y, Qin Z, Xiao R. Dietary intake of riboflavin and unsaturated fatty acid can improve the Multi-Domain cognitive function in Middle-Aged and elderly populations: A 2-Year prospective cohort study. Front Aging Neurosci. 2019;11:226.
20. Wang XA-O, Bakulski KM, Karvonen-Gutierrez CA, Park SK, Morgan D, Albin RL, Paulson HL. Blood-based biomarkers for Alzheimer's disease and cognitive function from mid- to late life. Alzheimers Dement. 2024;20(3):1807–14.
21. Sung CM, Lee TY, Chu H, Liu D, Lin HC, Pien LC, Jen HJ, Lai YJ, Kang XL, Chou KR. Efficacy of multi-domain cognitive function training on cognitive function, working memory, attention, and coordination in older adults with mild cognitive impairment and mild dementia: A one-year prospective randomised controlled trial. J Glob Health. 2023;13:04069.
22. Yu HA-O, Liu S, Dai P, Wang Z, Liu C, Zhang H. Effects of repetitive transcranial magnetic stimulation on gait and postural control ability of patients with executive dysfunction after stroke. Brain Sci. 2022;12(9):1185.
23. Petersen RC, Smith Ge Fau - Waring SC, Waring Sc Fau - Ivnik RJ, Ivnik Rj Fau - Tangalos EG, Tangalos Eg Fau - Kokmen E, Kokmen E. Mild cognitive impairment: clinical characterization and outcome. Arch Neurol. 1999; 56(3):303–308.
24. Guo Z, Yu H, Yang KA-OX, Feng WA-O, Liu M, Wang T, Xiao R. Quantitative determination of a series of oxysterols by an optimized LC-MS/MS analysis in different tissue types. Int J Mol Sci. 2024;26(1):77.
25. Bi XA-O, Li L, Xu R, Xing Z. Pathogenic factors identification of brain imaging and gene in late mild cognitive impairment. Interdiscip Sci. 2021;13(3):511–20.
26. Jessen F, Wolfsgruber S, Wiese B, Bickel H, Mösch E, Kaduszkiewicz H, et al. AD dementia risk in late MCI, in early MCI, and in subjective memory impairment. Alzheimers Dement. 2014;10(1):76–83.
27. Lin SY, Lin PC, Lin YC, Lee YJ, Wang CY, Peng SW, Wang PN. The clinical course of early and late mild cognitive impairment. Front Neurol. 2022;13:685636.
28. Zhang Y, Chen H, Li R, Sterling K, Song WA-OX. Amyloid β-based therapy for Alzheimer's disease: challenges, successes and future. Signal Transduct Target Ther. 2023;8(1):248.
29. Vasantharekha RA-O, Priyanka HP, Nair RS, Hima L, Pratap UP, Srinivasan AV, ThyagaRajan S. Alterations in immune responses are associated with dysfunctional intracellular signaling in peripheral blood mononuclear cells of men and women with mild cognitive impairment and Alzheimer's disease. Mol Neurobiol. 2024;61(5):2964–77.
30. Nelson ER, Wardell Se Fau - Jasper JS, Jasper Js Fau -, Park S, Park S, Fau - Suchindran S, Suchindran S et al. Fau - Howe MK, Howe Mk Fau - Carver NJ,. 27-Hydroxycholesterol links hypercholesterolemia and breast cancer pathophysiology. Science. 2013; 342(6162):1094–1098.
31. Liu Q, An Y, Yu H, Lu Y, Feng L, Wang C, Xiao R. Relationship between oxysterols and mild cognitive impairment in the elderly: a case-control study. Lipids Health Dis. 2016;15(1):177.
32. Arnal-Levron M, Chen Y, Fau - Delton-Vandenbroucke I, Delton-Vandenbroucke I, Fau - Luquain-Costaz C, Luquain-Costaz C. Bis(monoacylglycero) phosphate reduces oxysterol formation and apoptosis in macrophages exposed to oxidized LDL. Biochem Pharmacol. 2013;86(1):115–21.
33. Hartley A, Haskard D, Khamis R. Oxidized LDL and anti-oxidized LDL antibodies in atherosclerosis - Novel insights and future directions in diagnosis and therapy. Trends Cardiovasc Med. 2019;29(1):22–6.

34. Kunjathoor VV, Tseng Aa Fau - Medeiros LA, Medeiros La Fau -, Khan T, Khan T, Fau - Moore KJ, Moore KJ. beta-Amyloid promotes accumulation of lipid peroxides by inhibiting CD36-mediated clearance of oxidized lipoproteins. J Neuroinflammation. 2004; 1(1):23.
35. Zhao Z, Zhou H, Peng Y, Qiu CH, Sun QY, Wang F, Xie HN. Expression and significance of plasma 3-NT and ox-LDL in patients with Alzheimer's disease. Genet Mol Res. 2014;13(4):8428–35.
36. Murr J, Carmichael PH, Julien P, Laurin D. Plasma oxidized low-density lipoprotein levels and risk of Alzheimer's disease. Neurobiol Aging. 2014;35(8):1833–8.
37. Lu Y, Jiang H, Zhang H, Li R, Zhang Q, Luo D, Cai X, Li M. Serum oxidized low density lipoprotein serves as a mediator for the inverse relationship between serum d-ribose and cognitive performance in type 2 diabetic patients. Free Radic Biol Med. 2021;171:91–8.
38. Zhu G, Zhao J, Zhang H, Wang G, Chen W. Gut microbiota and its metabolites: Bridge of dietary nutrients and Alzheimer's disease. Adv Nutr. 2023;14(4):819–39.
39. Gao C, Li B, He Y, Huang P, Du J, He G, Zhang P, Tang H, Chen SA-O. Early changes of fecal short-chain fatty acid levels in patients with mild cognitive impairments. CNS Neurosci Ther. 2023;29(11):3657–66.
40. Malterud KE, Rydland KM. Inhibitors of 15-lipoxygenase from orange Peel. J Agric Food Chem. 2000;48(11):5576–80.
41. Ngouné B, Pengou M, Nouteza AM, Nanseu-Njiki CP, Ngameni E. Performances of alkaloid extract from Rauvolfia macrophylla Stapf toward corrosion Inhibition of C38 steel in acidic media. ACS Omega. 2019;4(5):9081–91.
42. Wang K, Feng X, Chai L, Cao S, Qiu F. The metabolism of Berberine and its contribution to the Pharmacological effects. Drug Metab Rev. 2017;49(2):139–57.
43. Chan KKP, Hui DSC. Antiviral therapies for influenza. Curr Opin Infect Dis. 2023;36(2):124–31.
44. Hsu KW, Lai JC, Chang JS, Peng PH, Huang CH, Lee DY, et al. METTL4-mediated nuclear N6-deoxyadenosine methylation promotes metastasis through activating multiple metastasis-inducing targets. Genome Biol. 2022;23(1):249.
45. Shen M, Li Y, Wang Y, Shao J, Zhang F, Yin G, Chen A, Zhang Z, Zheng S. N(6)-methyladenosine modification regulates ferroptosis through autophagy signaling pathway in hepatic stellate cells. Redox Biol. 2021;47:102151.
46. Li W, Deng ZA-O, Xiao S, Du Q, Zhang M, Song H, Zhao C, Zheng LA-O. Protective effect of vitexin against high fat-induced vascular endothelial inflammation through inhibiting trimethylamine N-oxide-mediated RNA m6A modification. Food Funct. 2024;15(13):6988–7002.
47. Ge P, Duan H, Tao C, Niu S, Hu Y, Duan R, Shen A, Sun Y, Sun W. TMAO promotes NLRP3 inflammasome activation of microglia aggravating neurological injury in ischemic stroke through FTO/IGF2BP2. J Inflamm Res. 2023;16:3699–714.
48. Liu K, He X, Huang J, Yu S, Cui M, Gao M, et al. Short-chain fatty acid-butyric acid ameliorates granulosa cells inflammation through regulating METTL3-mediated N6-methyladenosine modification of FOSL2 in polycystic ovarian syndrome. Clin Epigenetics. 2023;15(1):86.

Publisher's note